Doctoral Dissertation

Studies on Specific Properties of Li^+-Encapsulated [60]Fullerene $[Li^+@C_{60}](X^-)$ Arising from Internal Li^+

(内包リチウムイオンがもたらすリチウムイオン内包フラーレンの特異的物性に関する研究)

Hiroshi Ueno

January 2014

Division of Applied Chemistry
Graduate School of Engineering
Osaka University

Preface

The studies presented in this thesis have been carried out under the supervision by Prof. Dr. Takumi Oshima and Associate Prof. Dr. Ken Kokubo, Division of Applied Chemistry, Graduate School of Engineering, Osaka University during 2011-2014.

The objects of this thesis are the development of fundamental chemistry of lithium ion-encapsulated fullerene $Li^{+}@C_{60}$ focused on the derivatizations, kinetic study and ionic property. The author hopes that the described works in this thesis contributes to further development of endohedral fullerene chemistry and leads new application of fullerene family in materials chemistry.

Hiroshi Ueno

Division of Applied Chemistry

Graduate School of Engineering

Osaka University

Suita, Osaka

JAPAN

March 2014

Contents

General Introduction

1. Fullerenes

The first discovery of fullerenes which are the third carbon allotrope besides diamond and graphite was reported by Curl, Kroto, and Smalley in 1985,[1] and since then they have attracted much attention because of the unique closed-cage shape, reactivity, electrochemical property, and other various characteristics.[2] They have been most studied in the field of nanotechnology as superconducting materials, nanomedicines, organic electronics devices, and so on. Among all fullerene family like C_{60}, C_{70}, C_{82}, and other higher fullerenes, C_{60} is the most representative, abundant, and thus the most widely studied all over the world. Over the past 28 years from the discovery, although more than 50,000 papers and 6,000 patents have been published, there are still a lot of research projects undertaken in fullerene chemistry.

2. Endohedral Fullerenes

Due to the three-dimensional closed-cage structure, fullerenes have internal cavity space with ca. 0.4 nm diameter which can be inserted by small atoms, molecules, and ions. The insertion of any guests to a fullerene cage is one of the fundamental procedures to endow them with unique characteristic properties by way of supramolecular chemistry. The resulting products are called "endohedral fullerenes".[3] The first accomplishment of the synthesis was the insertion of La atom to C_{82} cage reported in 1985, just soon after the discovery of fullerenes.[4] Since La-encapsulated fullerene La@C_{82} was first isolated in 1991,[5,6] many studies on endohedral fullerenes have been devoted because of their unique electronic structures that are triggered by the interaction between the internal guest and the outer fullerene cage. In recent years, the synthetic procedures and the isolation processes have been widely developed.[7,8] In addition, a novel insertion method so-called "molecular surgery",[9] which includes the construction of a suitable orifice on the surface of an

	1	2	3	4	5	6	7	8	9	10	11	12	13	14	15	16	17	18
1	H																	He
2	Li	Be											B	C	N	O	F	Ne
3	Na	Mg											Al	Si	P	S	Cl	Ar
4	K	Ca	Sc	Ti	V	Cr	Mn	Fe	Co	Ni	Cu	Zn	Ga	Ge	As	Se	Br	Kr
5	Rb	Sr	Y	Zr	Nb	Mo	Tc	Ru	Rh	Pd	Ag	Cd	In	Sn	Sb	Te	I	Xe
6	Cs	Ba	*	Hf	Ta	W	Re	Os	Ir	Pt	Au	Hg	Tl	Pb	Bi	Po	At	Rn

La	Ce	Pr	Nd	Pm	Sm	Eu	Gd	Tb	Dy	Ho	Er	Tm	Yb	Lu

Figure 1. Elements encapsulated in fullerene cages. The colored cells mean that the atoms have been well-characterized by spectrometric or spectroscopic analyses, while the dotted cells mean their insufficient characterization.

empty fullerene cage, insertion of atoms or small molecules through it, and then restoration of the original fullerene cage retaining the encapsulated species, have been reported. Therefore the endohedral fullerene chemistry will be more active for the application especially in the field of organic electronics. Along the way, various kinds of endohedral fullerenes have been prepared (Figure 1).[10] There are some other endohedral fullerenes encapsulating H_2, H_2O, He/N, and clusters such as Sc_3N.[11]

3. Lithium Ion-Encapsulated [60]Fullerene $Li^+@C_{60}$

3-1. Synthesis and Purification of $Li@C_{60}$: The First Isolated Alkali-Metal Ion-Encapsulated Fullerene

Lithium-encapsulated fullerene $Li@C_{60}$ was first reported in 1996 by Campbell et al.[12] However, the formation of $Li@C_{60}$ was only suggested by the corresponding mass number (m/z =727), and the "encapsulation" was not confirmed by any spectroscopic and spectrometric measurements. In 2010 (14 years later since the first report), $Li@C_{60}$ was eventually isolated and well-characterized by Sawa and Tobita et al. as a $SbCl_6$ salt $[Li^+@C_{60}](SbCl_6^-)$.[10b] The synthesis was carried out by "plasma shower method" which was first performed in 1996 as the insertion procedure of potassium

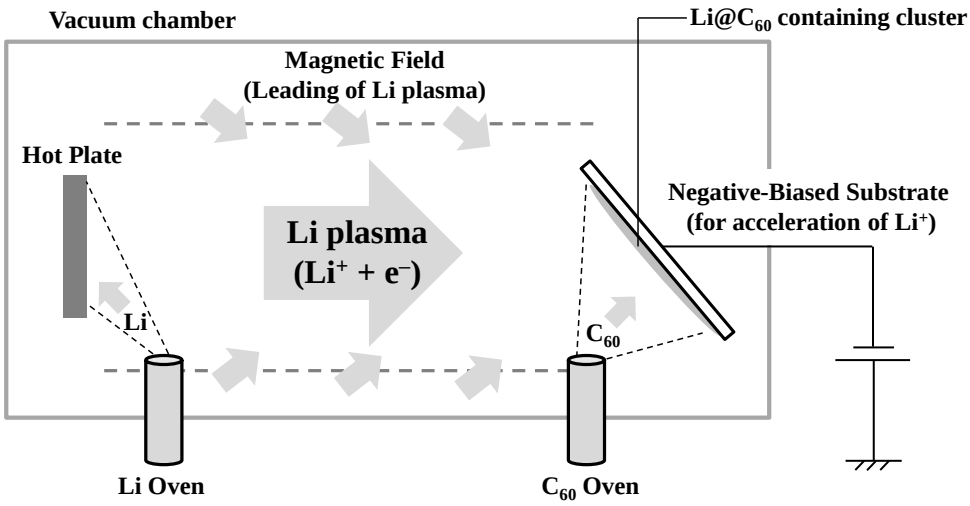

Figure 2. Schematic diagram of the plasma shower method.

to fullerene by Hatakeyama et al.[13] The schematic image of the method is shown in Figure 2. The Li@C_{60} was obtained as a cluster containing the desirable Li@C_{60} with empty C_{60}, solid lithium, and extra electron(s) (Scheme 1). In this stage, the content of Li@C_{60} is ca. 5% and it is difficult to isolate it by the current HPLC technique for the purification of endohedral fullerenes probably due to the strong charge transfer interaction between negatively charged Li@C_{60} cage and surrounding empty C_{60}. The purification was achieved by the oxidation using tris(4-bromophenyl)ammoniumyl hexachloroantimonate which is known as a strong one-electron oxidant to remove the extra electrons and to provide the counter anion $SbCl_6^-$ as shown in Scheme 1.[14] After the stable ion pair formation, the desirable pure $SbCl_6$ salt was isolated by recrystallization and submitted to X-ray structural analysis. This is the first isolated and structurally well-determined Li^+-encapsulated fullerene.

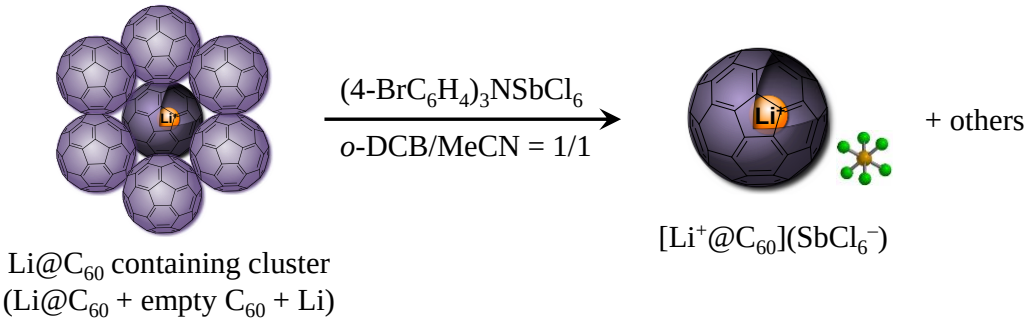

Scheme 1. Synthetic scheme to obtain the $SbCl_6$ salt [Li^+@C_{60}]($SbCl_6^-$).

3-2. Meaning of "Li@C_{60}" and "Li^+@C_{60}": Difference between General Endohedral Fullerene and the Present Li^+-Encapsulated Fullerene

The above two different notations, Li@C_{60} and Li^+@C_{60}, express the major difference between general endohedral fullerenes and the present Li^+-encapsulated fullerene. This point is significantly important for the Li^+@C_{60} chemistry. Figure 3 illustrates the difference between La@C_{82}, which is one of the major typical endohedral fullerenes, and Li^+@C_{60}. La@C_{82} has three electrons which are transferred from the encapsulated La atom, and thus the C_{82} cage becomes anionic.[15] On the other hand, due to its synthetic procedure and purification process of Li^+@C_{60}, it has "external counter anion" such as PF_6^- and thus the C_{60} cage is neutral. In other words, the former endohedral fullerene is considered as La^{3+}@C_{82}^{3-} while the latter one is general ion pair consisted of [Li^+@C_{60}^0] cation with an external counter anion PF_6^-. In addition, before the purification of above-mentioned cluster, the contained Li@C_{60} may have extra electrons, and thus the electronic state of its C_{60} cage may be somewhat anionic, which has been confirmed by ESR measurement (*vide infra*). To distinguish the purified "ionic" Li^+-encapsulated fullerene from the cluster as well as general endohedral metallofullerenes, two notations are required and suitably used, such as Li@C_{60} and Li^+@C_{60}.

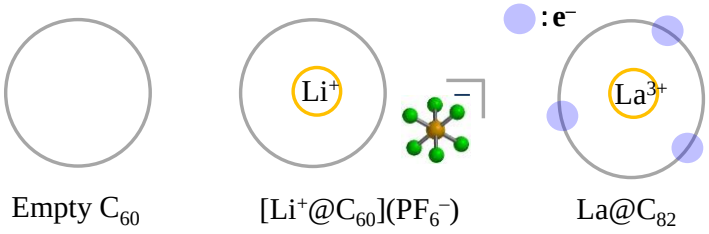

Figure 3. Difference of electronic state of their cages between La@C_{82} and [Li^+@C_{60}](PF_6^-).

3-3. Chemical Properties of Li^+@C_{60}

The remarkable properties of Li^+@C_{60} are (1) above-mentioned ionic nature and (2) the strongest electron acceptability among all endohedral fullerenes reported.

The ionic property in the view of its crystal structure was reported by Aoyagi et al. in 2012.[16] Li^+@C_{60} and the counter anion PF_6^- formed rock-salt-type crystal and the precise structural

information was reported by their study. Furthermore, the thermal motion of the encapsulated Li^+ was controlled by exchanging the counter anion. Figure 4 shows such difference in crystal structure between PF_6^- and $SbCl_6^-$ salts. This result implies that $Li^+@C_{60}$ is promising materials for molecular devices such as a single molecular memory.[17]

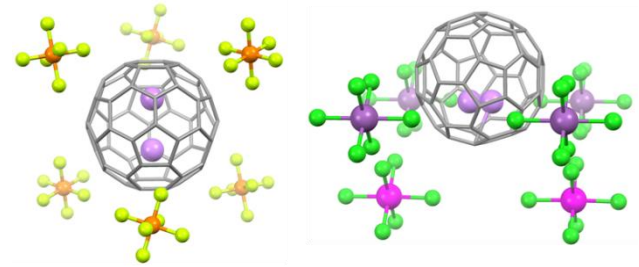

Figure 4. Crystal structure difference between $[Li^+@C_{60}](PF_6^-)$ (left) and $[Li^+@C_{60}](SbCl_6^-)$ (right).

The strong electron acceptability of $Li^+@C_{60}$ has been a mainstay of the study using the material. Cyclic voltammogram of $Li^+@C_{60}$ is shown in Figure 5a along with that of empty C_{60}. The first reduction potential which corresponds to LUMO of $Li^+@C_{60}$ is –0.39 V vs Fc/Fc^+ which is ca. 0.7 V higher than that of empty C_{60}. Considering their similar absorption spectra as shown in Figure 5b, $Li^+@C_{60}$ has essentially the same HOMO–LUMO energy gap with empty C_{60}, and the all corresponding energy level of MOs are ca. 0.7 eV lower than that of empty C_{60}. Thus, $Li^+@C_{60}$ can apply to *n*-type material combined with an appropriate *p*-type molecule which cannot be an electron donor for the less electron accepting empty C_{60}.

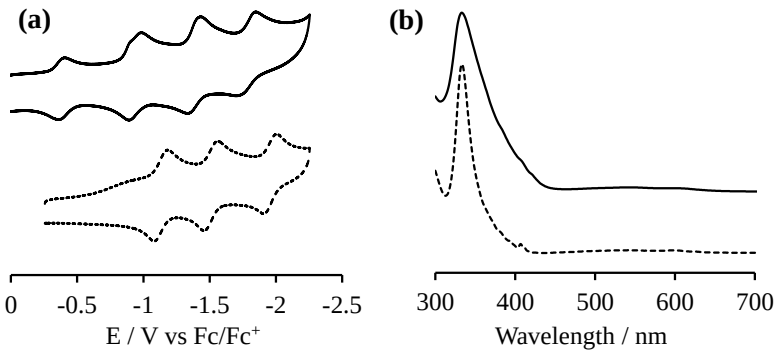

Figure 5. Cyclic voltammograms in *o*-DCB containing 50 mM Bu_4NPF_6 (a) and UV-vis absorption spectra in *o*-DCB (b) of $Li^+@C_{60}$ (solid line) and empty C_{60} (dotted line).

3-4. Variety of Counter Anion

As compared with empty C_{60}, the solubility of the typical salt $[Li^+@C_{60}]PF_6^-$ is generally lower, which is a drawback to this compound. To improve the problem, anion exchanging was first

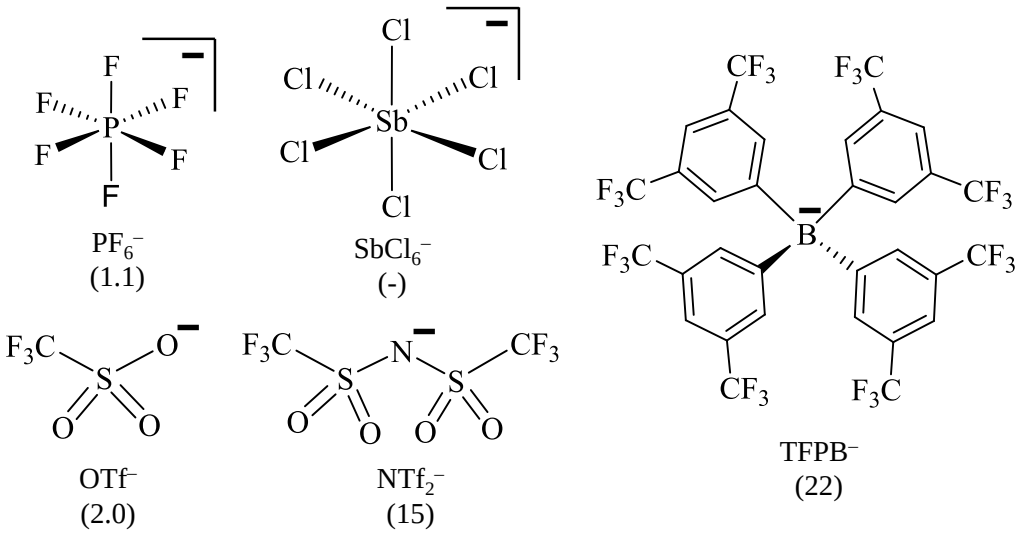

Figure 6. Variety of counter anions of $Li^+@C_{60}$. The values in parentheses are solubility to dichloromethane (mg/mL).

performed by Matsuo et al. in 2013.[18] The reported $Li^+@C_{60}$ salts are shown in Figure 6 along with their solubility to CH_2Cl_2. As mentioned above, the properties of $Li^+@C_{60}$ salts can be affected by the anion exchanging due to the electrostatic interaction between internal Li^+ and external counter anion. In addition, the ionic properties are somewhat related to the size and negative charge of the counter anion. In this point of view, anion exchanging is one of the modifications of $Li^+@C_{60}$, and the development of anion-exchanging process has been strongly demanded.

4. Chemical Modification of Li^+-Encapsulated Fullerene

Chemical functionalization on the fullerenyl cage is also a powerful tool to provide a variety of unique properties to the fullerenes. A great number of fullerene derivatives have been synthesized and examined their functions especially in the field of organic device and medicinal/pharmaceutical studies.[19] Li^+@PCBM was the first $Li^+@C_{60}$ derivative reported by Matsuo et al. in 2012.[20] However, there are only a few reports concerning the functionalization of the novel endohedral fullerene. To develop the chemistry of $Li^+@C_{60}$, derivatizations, studies on the reactivity, and application of the resulting compounds are quite important but stagnant as compared with the study of empty and other endohedral fullerenes.

5. Synopsis of This Thesis

Because of the short period from the discovery of Li^+-encapsulated [60]fullerene, the studies on the novel endohedral fullerene are insufficient as compared with the present fullerene-based materials. For the future development and application, the study on the basic properties of the $Li^+@C_{60}$ cannot be missed, playing a significant role in the field of fullerene chemistry.

As mentioned above, $Li^+@C_{60}$ has mainly two unique properties, ionicity and strong electron acceptability which are the key words for the differentiation of $Li^+@C_{60}$ from empty and other endohedral fullerenes. In this thesis, much attention is focused on these properties peculiar to an internal Li^+ in the view of chemical functionalization, reactivity, and ionic properties.

In chapter 1, multihydroxylated derivatives of $[Li^+@C_{60}](PF_6^-)$ and/or $Li@C_{60}$ cluster, their characterization, and aggregation behavior in polar solvent are reported. In addition, unprecedentedly high site-selectivity observed for the hydroxylation reaction of the PF_6^- salt was also revealed.

In chapter 2, synthesis and characterization of Diels-Alder product obtained by the reaction of $Li^+@C_{60}$ with 1,3-cyclohexadiene was described. Furthermore, enhanced reactivity of $Li^+@C_{60}$ was kinetically studied and the reasons for the acceleration were also mentioned.

In chapter 3, the ionic conductivity of two kinds of $Li^+@C_{60}$ salts, PF_6^- and NTf_2^- salts, were measured in organic solvents. Based on the observed relatively higher ionic conductivity, $Li^+@C_{60}$ monovalent radical anion was synthesized by a facile electrochemical procedure and characterized mainly by ESR and Raman spectroscopy. The difference between the starting salt form Li^+-encapsulated fullerene and synthesized $Li^+@C_{60}^{\bullet-}$ was particularly discussed.

References

[1] Kroto, H. W.; Heath, J. R.; O'Brien, S. C.; Curl, R. F.; Smalley, R. E. *Nature* **1985**, *318*, 162.

[2] (a) Haddron, R. C. *Acc. Chem. Res.* **1992**, *25*, 127. (b) Haddron, R. C.; Brus, L. E.; Raghavachari, K. *Chem. Phys. Lett*. **1986**, *125*, 459. (c) Haymet, A. D. J. *Chem. Phys. Lett.* **1985**, *122*, 421. (d) Wudl, F. *Acc. Chem. Res.* **1992**, *25*, 157. (e) Kroto, H. W.; Allaf, A. W.; Balm, S. P. *Chem. Rev.* **1991**, *91*, 1213. (f) Kratschmer, W.; Lamb, L. D.; Fostiropoulos, K.; Huffman, D. R. *Nature* **1990**, *347*, 354.

[3] (a) Shinohara, H. *Rep. Prog. Phys.* **2000**, *63*, 843. (b) *Endofullerenes: A New Family of Carbon Clusters*; Akasaka, T., Nagase, S., Eds.; Kluwer: Dordrecht, The Netherlands, 2002.

[4] Heath, J. R.; O'Brien, S. C.; Zhang, Q.; Liu, Y.; Curl, R. F.; Tittel, F. K.; Smalley, R. E. *J. Am. Chem. Soc.* **1985**, *107*, 7779.

[5] Chai, Y.; Guo, T.; Jin, C.; Haufler, R. E.; Chibante, L. P. F.; Fure, J.; Wang, L.; Alford, J. M.; Smalley, R. E. *J. Phys. Chem.* **1991**, *95*, 7564.

[6] The denotation "@" is used to describe the encapsulation of the atom listed to the left of the @ symbol by the fullerene cage.

[7] Okada, H.; Komuro, T.; Sakai, T.; Matsuo, Y.; Ono, Y.; Omote, K.; Yokoo, K.; Kawachi, K.; Kasama, Y.; Ono, S.; Hatakeyama, R.; Kaneko, T.; Tobita, H. *RSC Advances* **2012**, *2*, 10624.

[8] Akiyama, K.; Hamano, T.; Nakanishi, Y.; Takeuchi, E.; Noda, S.; Wang, Z.; Kubuki, S.; Shinohara, H. *J. Am. Chem. Soc.* **2012**, *134*, 9762.

[9] Komatsu, K.; Murata, M.; Murata, Y. *Science* **2005**, *307*, 238.

[10] Studies on major endohedral fullerenes: (a) He-encapsulated fullerene: Morinaka, Y.; Sato, S.; Wakamiya, A.; Nikawa, H.; Mizorogi, N.; Tanabe F.; Murata, M.; Komatsu, K.; Furukawa, K.; Kato, T.; Nagase, S.; Akasaka, T.; Murata, Y. *Nat. Commun*. **2013**, *4*, 1554. (b) Li^+-encapsulated fullerene: Aoyagi, S.; Nishibori, E.; Sawa, H.; Sugimoto, K.; Takata, M.; Miyata, Y.; Kitaura, R.; Shinohara,

H.; Okada, H.; Sakai, T.; Ono, Y.; Kawachi, K.; Yokoo, K.; Ono, S.; Omote, K.; Kasama, Y.; Ishikawa, S.; Komuro, T.; Tobita, H. *Nat. Chem*. **2010**, *2*, 678. (c) N atom-encapsulated fullerene: Murphy, T. A.; Pawlik, Th.; Weidinger, A.; Höhne, M.; Alcala, R.; Spaeth, J.-M. *Phys. Rev. Lett*. **1996**, *77*, 1075. (d) Ca-encapsulated fullerene: Xu, Z.; Nakane, T.; Shinohara, H. *J. Am. Chem. Soc.* **1996**, *118*, 2293. (e) Y-encapsulated fullerene: Kikuchi, K.; Nakao, Y.; Suzuki, S.; Achiba, Y.; Suzuki, S.; Maruyama, Y. *J. Am. Chem. Soc*. **1994**, *116*, 9367. (f) Ce-encapsulated fullerene: Suzuki, T.; Kikuchi, K.; Oguri, F.; Nakao, Y.; Suzuki, S.; Achiba, Y.; Yamamoto, K.; Funasaka, H.; Takahashi, T. *Tetrahedron* **1996**, *52*, 4973. (g) Ga-encapsulated fullerene: Kikuchi, K.; Kobayashi, K.; Sueki, K.; Suzuki, S.; Nakahara, H.; Achiba, Y.; Tomura, K.; Katada, M. *J. Am. Chem. Soc*. **1994**, *116*, 9775.

[11] (a) H_2-encapsulated fullerene: Komatsu, K.; Murata, M.; Murata, Y. *Science* **2005**, *307*, 238. (b) H_2O-encapsulated fullerene: Kurotobi, K.; Murata, Y. *Science* **2011**, *333*, 613. (c) Nitride cluster-encapsulated fullerene: Stevenson, S.; Rice, G.; Glass, T.; Harich, K.; Cromer, F.; Jordan, M. R.; Craft, J.; Hadju, E.; Bible, R.; Olmstead, M. M.; Maitra, K.; Fisher, A. J.; Balch, A. L.; Dorn, H. C. *Nature* **1999**, *401*, 55.

[12] Tellgmann, R.; Krawez, N.; Lin, S.-H.; Hertel, I. V.; Canmpbell, E. E. B. *Nature* **1996**, *382*, 407.

[13] Hirata, T.; Hatakeyama, R.; Mieno, T.; Sato, N. *J. Vac. Sci. Technol. A* **1996**, *14*, 615.

[14] Connelly, N. G.; Geiger, W. E. *Chem. Rev.* **1996**, *96*, 877.

[15] (a) Johnson, R. D.; Vries, M. S.; Salem, J.; Bethune, D. S.; Yannoni, C. S. *Nature* **1992**, *355*, 239. (b) Nagase, S.; Kobayashi, K. *J. Chem. Soc., Chem. Commun.* **1994**, 1837.

[16] Aoyagi, S.; Sado, Y.; Nishibori, E.; Sawa, H.; Okada, H.; Tobita, H.; Kasama, Y.; Kitaura, R.; Shinohara, H. *Angew. Chem. Int. Ed.* **2012**, *51*, 3377.

[17] (a) Yasutake, Y.; Shi, Z.; Okazaki, T.; Shinohara, H.; Majima, Y. *Nano Lett*. **2005**, *5*, 1057. (b) Iwamoto, M.; Ogawa, D.; Yasutake, Y.; Azuma, Y.; Umemoto, H.; Ohashi, K.; Izumi, N.; Shinohara,

H.; Majima, Y. *J. Phys. Chem. C* **2010**, *114*, 14704. (c) Nuttall, C. J.; Hayashi, Y.; Yamazaki, K.; Mitani, T.; Iwasa, Y. *Adv. Mater.* **2002**, *14*, 293.

[18] Okada, H.; Matsuo, Y. *Full. Nanotub. Carbon Nanostruct.* **2013**, In press.

[19] Representative functionalization reactions of fullerenes: (a) Bingel, C. *Chem. Ber.* **1993**, *126*, 1957. (b) Maggini, M.; Scorrano, G.; Prato, M. *J. Am. Chem. Soc.* **1993**, *115*, 9798. (c) Sawamura, M.; Iikura, H.; Nakamura, E. *J. Am. Chem. Soc.* **1996**, *118*, 12850. (d) Suzuki, T.; Li, Q.; Khemani, K. C.; Wudl, F. *J. Am. Chem. Soc.* **1992**, *114*, 7301. (e) Prato, M.; Li, Q. C.; Wudl, F. *J. Am. Chem. Soc*. **1993**, *115*, 1148. (f) Nakamura, Y.; Okawa, K.; Matsumoto, M.; Nishimura, J. *Tetrahedron* **2000**, *56*, 5429. (g) Nakamura, Y.; Takano, N.; Nishimura, T.; Yashima, E.; Sato, M.; Kubo, T.; Nishimura, J. *Org. Lett*. **2001**, *3*, 1193.

[20] Matsuo, Y.; Okada, H.; Maruyama, M.; Sato, H.; Tobita, H.; Ono, Y.; Omote, K.; Kawachi, K.; Kasama, Y. *Org. Lett.* **2012**, *14*, 3784.

Chapter 1:
Synthesis of Multihydroxylated Li^+-Encapsulated Fullerene

As mentioned in general introduction, chemical functionalization of $Li^+@C_{60}$ is important study to develop the novel endohedral fullerene chemistry. In this chapter, the author presents the multihydroxylation of $Li^+@C_{60}$ and several properties of the resulting Li^+-encapsulated multihydroxylated fullerene as well as the unique reactivity of $Li^+@C_{60}$. For this examination, $[Li^+@C_{60}](PF_6^-)$ and $Li@C_{60}$ containing cluster were used as the starting materials.

Chapter 1-1. Hydroxylation of $Li@C_{60}$ Cluster

1. Introduction

Multihydroxylated fullerenes, so-called fullerenol $C_{60}(OH)_n$, have attracted considerable attention owing to their prominent hydrophilicity, bioactivity, and unique conductivity.[1,2] Various types of synthetic procedures, and thus, variously hydroxylated fullerenols (e.g., n = 12, 16, 24, 36, and 44 as estimated average structures), have been reported.[3] Although some metal-encapsulated endohedral fullerene derivatives have been known, only a few reports on gadolinium-encapsulated fullerenol $Gd@C_n(OH)_m$ (n = 60 and 82; m = 24), but no report on other-metal-encapsulated fullerenol, have been reported.[4]

As a continuing interest of our studies on the synthesis and particle size analysis of fullerenols, the author herein focuses on both the ionicity of $Li@C_{60}$ and the hydrophilicity of fullerenols, as the ionicity seems to be more enhanced in polar solvents to be applicable as new materials in the field of materials and life sciences. In this study, the author synthesized lithium-encapsulated fullerenol $Li@C_{60}(OH)_{18}$ through the hydroxylation of $Li@C_{60}$ using fuming sulfuric acid and investigated the effects of encapsulated lithium cations on the physicochemical properties and the aggregation

behavior in polar solvent in comparison with those of the similar but reference fullerenol $C_{60}(OH)_{16}$.

2. Results and Discussion

Because Li@C_{60} as-purchased was a cluster composed of lithium-encapsulated C_{60} anion radicals (ca. 5%) surrounded by neutral C_{60} molecules (ca. 95%), the sample was washed with *o*-dichlorobenzene beforehand to prepare a Li@C_{60}-rich cluster. The laser desorption ionization time of flight (LDI-TOF) mass spectrum of the pre-treated sample showed an increasing intensity of the Li@C_{60} peak (*m/z* = 727) relative to the C_{60} peak (*m/z* = 720) (Figure 1). Hydroxylation of Li@C_{60} cluster was carried out using the reported procedures under optimized reaction conditions (Scheme 1).[3a] The reaction with fuming sulfuric acid, followed by the hydrolysis of generated polycyclosulfated intermediate, took longer

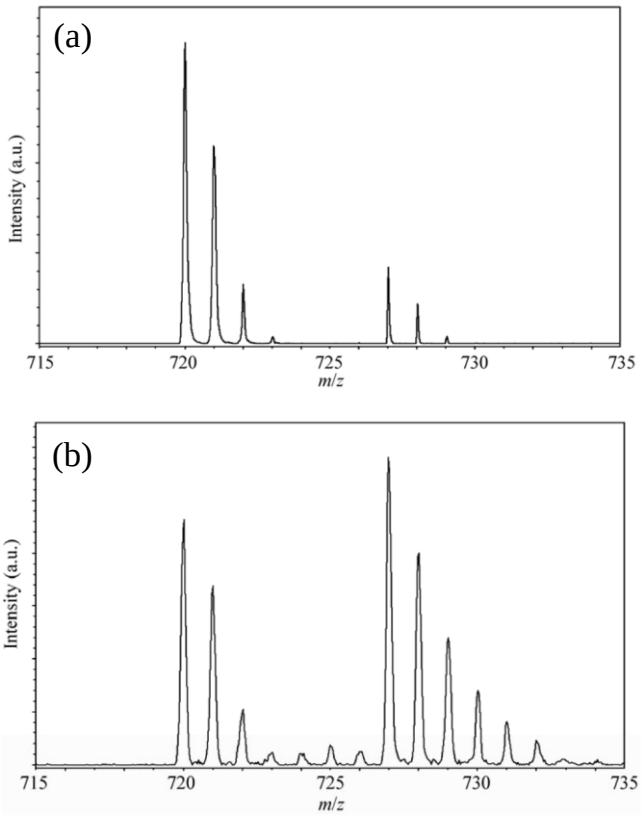

Figure 1. Positive mode LDI-TOF mass spectra of (a) Li@C_{60} cluster as purchased and (b) after washing with *o*-DCB.

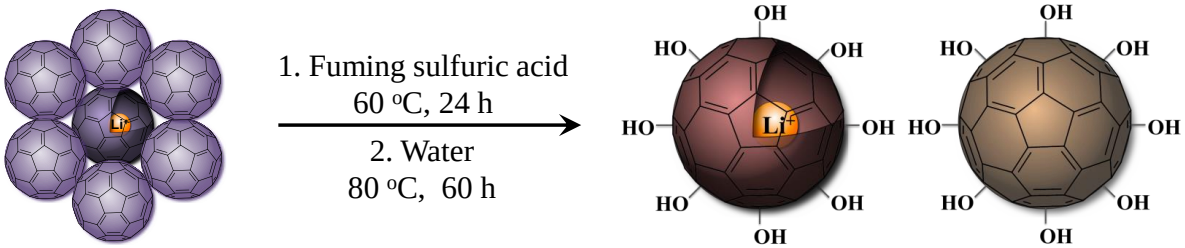

Li@C_{60} containing cluster
(Li@C_{60} + empty C_{60} + Li)

A mixture of Li^+@$C_{60}(OH)_{18}$ and empty $C_{60}(OH)_{18}$
(No cluster formation)

Scheme 1. Synthesis of Li@$C_{60}(OH)_n$.

time as compared with that of the pristine C_{60} due to the persistent cluster aggregation under the present heterogeneous solid/liquid reaction conditions. However, the oxidative fuming sulfuric acid may be effective in removing the electrons from the anionic cluster to negate the charge transfer interaction between $Li^+@C_{60}^{-\bullet}$ and empty C_{60}. The number of introduced hydroxyl group of the obtained fullerenol amounts to ca. 18 on 24 h sulfurization. Incidentally, the prolonged reaction time (60 h) provided essentially the same number of introduced hydroxyl group, implying almost the completion of sulfurization on 24 h treatment.

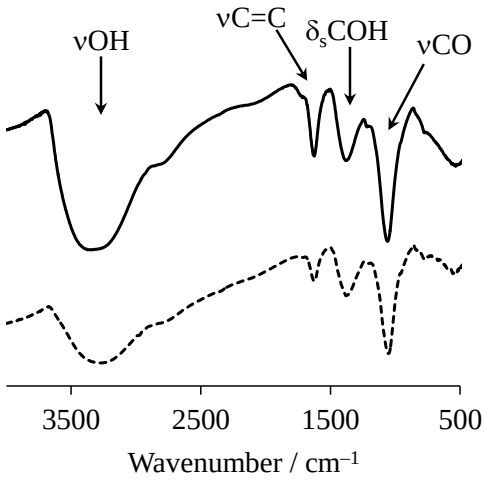

Figure 2. IR spectra (KBr pellet method) of the product (solid) and reference fullerenol $C_{60}(OH)_{16}$ (dotted).

The lithium-encapsulated fullerenol obtained was characterized through IR, a thermogravimetric analysis (TGA), and an elemental analysis, in the same manner as previously reported for $C_{60}(OH)_{36}$ and $C_{60}(OH)_{44}$.[3i,3j] The IR spectrum of the product is shown in Figure 2 along with that of the reference fullerenol $C_{60}(OH)_{16}$ synthesized independently by the same fuming sulfuric acid method. With a broad νO–H band at 3400 cm^{-1}, the spectra showed three characteristic bands at 1055, 1380, and 1625 cm^{-1} assignable to νC–O, δ_sC–O–H, and νC=C absorptions, respectively. These four broad bands have been invariably reported as diagnostic absorptions for various fullerenols.

The encapsulated Li^+ was clearly detected by ^{7}Li NMR spectroscopy. In the spectrum obtained in DMSO-d_6, a broad peak was observed in the range of −15 to −19 ppm along with a sharp signal near 0 ppm (integration ratio: 92/8) relative to LiCl in D_2O as an external standard (Figure 3). The latter signal can be attributable to the external Li^+ as a contaminant found in the starting cluster because this peak was sharp and not shifted on account of the free state of external Li^+. On the other hand, the peak attributable to the encapsulated Li^+ was highly broadened and up-field shifted

because the relevant fullerenol was a mixture of isomers with slightly different numbers of hydroxyl groups.

The chemical shift of the encapsulated Li^+ was found to be more shielded than previously reported value of –10.5 ppm for $[Li^+@C_{60}][SbCl_6^-]$ salt in *o*-dichlorobenzene-d_4/acetonitrile-d_3 by Sawa and Tobita *et al*.[5] This abnormal upfield shift of our sample may be caused by i) the enhanced π-electron ring current and/or ii) the increased diamagnetic shielding by some possible negative charge. It is not strange to assume that the inner Li^+ would induce the counter negative charge on C_{60} surface and/or on the hydroxyl group (*vide infra*). The latter case would result in the deprotonation to give fullerenoxide $C_{60}O^-$ anion which can be stabilized by the internal Li^+ through the C_{60} cage. Keeping this in mind, we have made the theoretical calculation to know how the lithium cation behaves in the anionic fullerene cage and is affected by the π-electron ring current (Figure 4). A model compound used is a Li^+

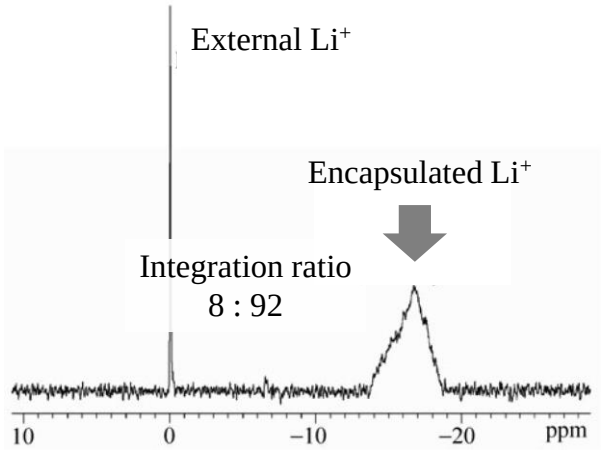

Figure 3. ^{7}Li NMR spectrum of the product in DMSO-d_6. The sharp signal at ca. 0 ppm is derived from the impurity of nonencapsulated Li^+ in the starting material (integration ratio: 92/8 for encapsulated/external). A D_2O solution of LiCl was used as an external standard.

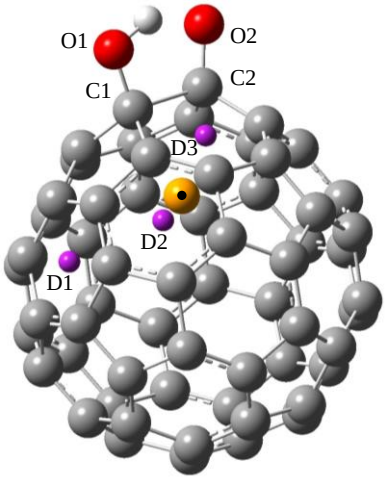

Bond	Distance (Å)
C1–O1	1.36
C2–O2	1.31
O1–Li^+	3.58
O2–Li^+	3.57
D1–Li^+	3.16
D2–Li^+	2.68
D3–Li^+	1.78
Cf.[a)]	2.24–2.45
Position	**Ring current (NICS)**
D1	–4.80
D2	–5.87
D3	+4.49
C60	–2.41

[a] The distances between the Li^+ and the six carbon atoms of $[Li^+@C_{60}](SbCl_6^-)$.

Figure 4. Theoretical calculation (B3LYP/6-31G* method) of the location of encapsulated lithium cation and of NICS (GIAO/B3LYP/6-31G*) on the center of 6-membered ring near the modified carbon atoms calculated for model $Li^+@C_{60}(O^-)(OH)$.

encapsulated monohydroxylated fullerenoxide anion ($C_{60}(O^-)(OH)$). It was found that π-electron ring current of fullerene cage was significantly reduced at the OH-substituted non-aromatic 6-membered rings but somewhat enhanced at other hexagonal rings. The calculation also showed that the Li^+ was positioned in the proximity of the negatively charged fullerenoxide moiety. This strongly suggests the upfield chemical shift of Li^+ is mainly caused by the increased diamagnetic field due to the closely located charge density rather than the ring current effect.

By contrast, rather reduced upfield shift of $[Li^+@C_{60}][SbCl_6^-]$ can be ascribed to the usual diamagnetic field induced by π-conjugated system not by the more remote and highly charge-dispersed counter anion $SbCl_6^-$ which would also be more separated by solvation.

The average structure of the product was appropriately determined by an elemental analysis and water-content measurement using TGA as $Li@C_{60}(OH)_{18}\cdot 6H_2O$ (Table 1). To estimate the molar ratio of encapsulated/empty fullerenol, the total amount of lithium involved was quantitatively measured using inductively coupled plasma atomic emission spectrometry (ICP-AES) analysis. Before the measurement, the present mixed fullerenol sample was completely degraded by heating it at 100 °C in concentrated nitric acid for 1 hour, followed by the addition of 30% hydrogen peroxide and further heating, to release the Li^+ from the C_{60} cage, and the obtained clear aqueous solution was then used for the analysis. Coupled with the result of ^7Li NMR spectroscopy, the molar ratio of $Li@C_{60}(OH)_{18}$ to empty $C_{60}(OH)_{18}$ was calculated as 12:88. As a result, it seems that pre-washing by *o*-dichlorobenzene somewhat increases the amount of Li^+ encapsulated C_{60} on judging from the 5% content of starting cluster sample. The elemental analysis provided a good consistency with the calculated value for a mixture (12:88) of $Li@C_{60}(OH)_{18}\cdot 6H_2O$ and $C_{60}(OH)_{18}\cdot 6H_2O$ (Table 1).

Table 1. Elemental analysis, water content, and average structure of the product.

Average structure	Elemental analysis (%)[a]	Water content (Wt %)[a,b]
Product	C: 62.91, H: 2.48	9.5
$Li@C_{60}(OH)_{18}\cdot 6H_2O$	(C: 63.12, H: 2.65)	(9.5)
$C_{60}(OH)_{18}\cdot 6H_2O$	(C: 63.50, H: 2.66)	(9.5)
Li@:empty = 11:88[c]	(C: 63.45, H: 2.66)	(9.5)

[a] Values in parentheses are calculated data. [b] Determined by thermogravimetric analysis. [c] A mixture of $Li@C_{60}(OH)_{18}\cdot 6H_2O$ and $C_{60}(OH)_{18}\cdot 6H_2O$ in a ratio of 12:88

Furthermore, we also confirmed the encapsulation of the lithium cation in the fullerene cage using matrix-assisted laser desorption ionization time of flight (MALDI-TOF) mass spectroscopy. The peaks observed at *m/z* = 897, 913, and 930 attributed to $Li@C_{60}(OH)_{10\text{-}12}$ which are intermediary fullerenols in the reaction, were detected in the negative mode of the MALDI-TOF mass spectroscopy, although the clear mass spectra for the final product (n = 18) were not obtained (Figure 5). This is consistent with our previous observation that the fullerenols with up to ca. 14 hydroxyl groups could only be detected by mass spectroscopy due to the possible degradation of more highly hydroxylated fullerenols under the ionization condition.[3i] The peaks at m/z = 941, 958, and 975 assignable to the empty $C_{60}(OH)_{13\text{-}15}$ were also detected as shown in Figure 5.

The solid-state electron spin resonance (ESR) spectrum of the starting $Li@C_{60}$ cluster showed a clear signal (g = 2.0024) at 298 K, suggesting the existence of $C_{60}^{-\bullet}$ anion radical,[6]

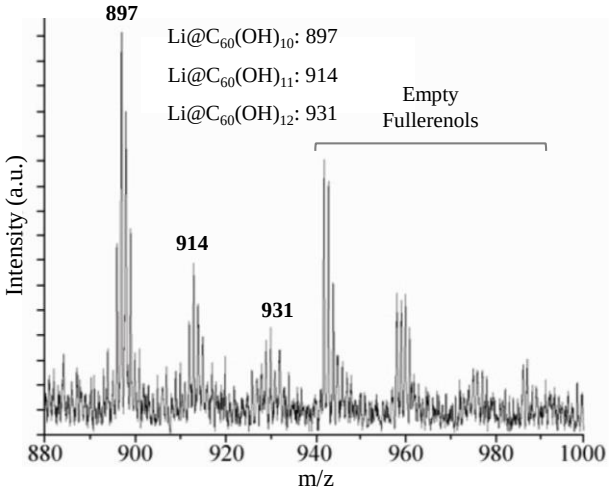

Figure 5. Negative mode MALDI-TOF mass spectrum of the intermediate product obtained for the reaction mixture in the early stages of the synthesis of $Li@C_{60}(OH)_{18}$.

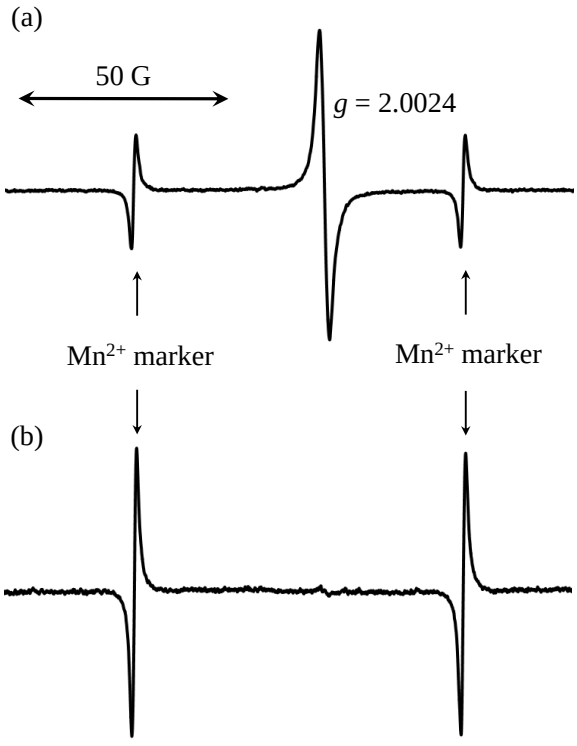

Figure 6. Solid state ESR spectra of (a) the $Li@C_{60}$ cluster and (b) the product at 298 K calibrated by using Mn^{2+} marker.

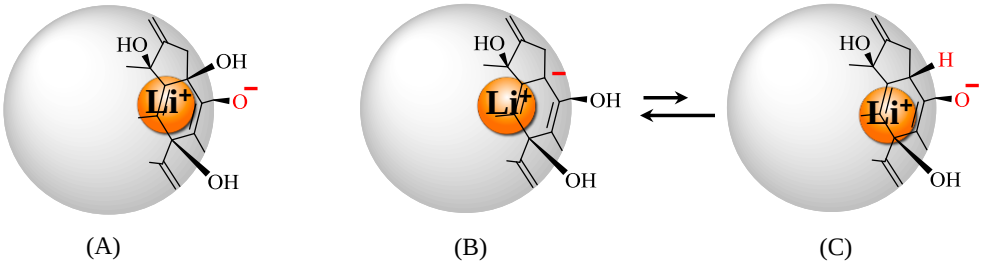

(A) (B) (C)

Figure 7. Possible chemical structures (A-C) of Li@$C_{60}(OH)_{18}$.

while that of our fullerenol did not show the corresponding signal (Figure 6). Some highly hydroxylated fullerenols are known to show the similar ESR signal (g = 2.0026 and 2.0033 for $C_{60}H_2(OH)_{24}$ and $C_{60}(OH)_{36}$, respectively).[3i,7] Thus, the absence of an ESR signal for the present fullerenol strongly indicates that the counter anion is not the $C_{60}^{-\bullet}$ anion radical but the proposed fullerenoxide anion (*vide infra*).

Three possible chemical structures (A-C) of the Li^+ encapsulated fullerenol salts are depicted in Figure 7. In the case of A with an even number of hydroxyl groups, one –OH group is deprotonated to fullerenoxide anion which can favorably interact with inner Li^+ (Figure 7A). The similar fullerenoxide form with no inner cation is reported for fullerenol Na^+ salt with a molecular formula of $Na^+_n[C_{60}O_x(OH)_y]^{n-}$.[7] By contrast, an odd number of –OH groups (though the incorporation of which is less favorable owing to the inevitable generation of unpaired electron, or anion/cation center) can also form a similar salt C through a possible proton transfer to the anion center of the fullerenyl carbon of the structure B (Figure 7). The equilibrium shift is dependent on the number of hydroxyl groups (the acidity of the protons) as well as the degree of π-conjugation. It should be emphasized that the electronic structure of $Li^+@C_{60}(O^-)(OH)_n$ allows the outer anionic behavior of this spherical compound in a solution as well as in solid state due to the intriguing electrostatic stabilization by the inner-captured Li^+. Therefore, we can refer to this compound as 'cation-encapsulated anion nanoparticle'.

Interestingly, notable aggregation behavior was observed in the particle-size measurement of my

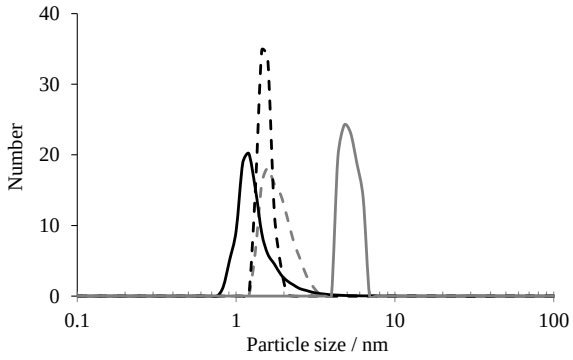

Compound	Average particle size / nm	
	In DMSO/H_2O (3/7 *v*/*v*)	In DMSO
Product	1.25 (0.120)[a]	1.47 (0.042)[a]
Ref. $C_{60}(OH)_{16}$	4.97 (0.066)[a]	1.73 (0.088)[a]

[a] Values in parentheses are standard deviations of the measurement.

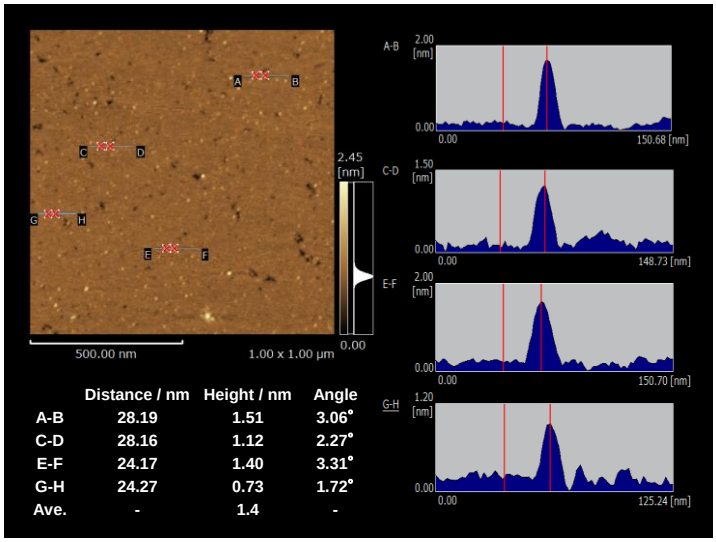

	Distance / nm	Height / nm	Angle
A-B	28.19	1.51	3.06°
C-D	28.16	1.12	2.27°
E-F	24.17	1.40	3.31°
G-H	24.27	0.73	1.72°
Ave.	-	1.4	-

Figure 8. Particle size distribution of the product (black) and reference fullerenol $C_{60}(OH)_{16}$ (gray) in DMSO/H_2O (3/7 v/v, solid line) and in DMSO (dotted line) measured by the induced grating method (left) and SPM particle analysis for the product (right).

fullerenol vs reference fullerenol $C_{60}(OH)_{16}$. To precisely estimate the particle size, the author used an Induced Grating (IG) method, which was properly designed for measurement in a single-nano (1–10 nm) region.[8] Although the present sample and reference $C_{60}(OH)_{16}$ showed almost the same small and narrow particle-size distribution (ca. 1.5 nm) in a DMSO solution, a drastic change was observed by the addition of water so as to increase the solvent polarity. The DMSO/water (3/7 v/v) solution of the reference $C_{60}(OH)_{16}$ exhibited aggregation behavior (ca. 5 nm), owing to the hydrophobic interaction between the unhydroxylated C_{60} surfaces as previously known, while the present fullerenol retained its original molecular size (ca. 1.3 nm) (Figure 8, left). A similar particle size of ca. 1.4 nm was also observed for this sample on a scanning

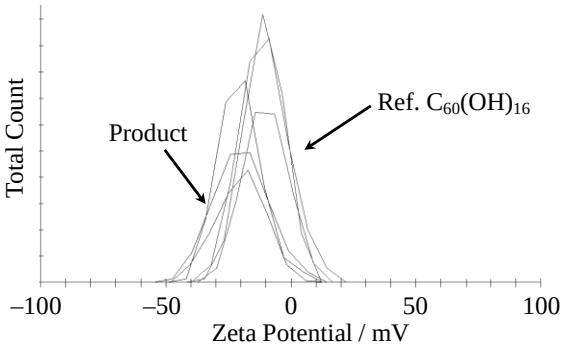

Compound	Average zeta potential / mV
$Li@C_{60}(OH)_{18}$	-20.0 (0.231)[a]
Ref. $C_{60}(OH)_{16}$	-10.4 (0.396)[a]

[a] Values in parentheses are standard deviations of the measurement.

Figure 9. Zeta potential distribution of the product and reference $C_{60}(OH)_{16}$ in DMSO.

probe microscopy (SPM) measurement, achieved by applying the diluted DMSO solution to a mica plate and drying it (Figure 8, right).[3j]

Why does my lithium encapsulated fullerenol retain its intrinsic molecular size in contrast to aggregated reference $C_{60}(OH)_{16}$? The author measured the zeta potential of the two types of fullerenols in DMSO to determine the surface charge density (Figure 9). The former particle showed a more negative potential (−20.0 mV) than the latter one (−10.4 mV). It should be noted that the product was a mixture of Li^+ encapsulated and empty fullerenols in a molar ratio of 12:88. The remarkable influence of the existence of only 12% $Li@C_{60}(OH)_{18}$ was observed, and thus, the observed potentials suggest that $Li@C_{60}(OH)_{18}$ seems to play as negatively charged anion particles as the author proposed.

3. Conclusions

In summary, the author synthesized $Li@C_{60}(OH)_{18}•6H_2O$ using fuming sulfuric acid and characterized its structure, particularly to confirm the lithium encapsulation, through ^7Li NMR and MALDI-TOF mass spectroscopy as well as through a quantitative analysis of the lithium content using ICP-AES. The solid-state ESR and particle-size measurements using the IG method showed anionic behavior with no external counter cations, revealing the differences in its properties from those of reference $C_{60}(OH)_{16}$. This new nanomaterial is expected to be applied in not only the electrochemical field but also the biochemical and medical fields, on account of their hydrophilicity.

4. Experimental Section

General Procedure

$Li@C_{60}$ was obtained from Idea International Corporation. All other reagents were commercially available and used without further purification. Laser desorption ionization and matrix assisted laser desorption ionization time-of-flight mass spectra (LDI-TOF-MS and MALDI-TOF-MS) were

measured on a Bruker autoflex III. The ^{7}Li nuclear magnetic resonance (NMR) spectra were recorded at 233.112 MHz with a relaxation time of 7 s (to ensure the quantitative measurement, we measured each relaxation time of both external and encapsulated Li species which gave values of ca. 6 s and less than 1 s, respectively) on a Varian Unity Inova 600. The NMR spectra are referred to LiCl/D_2O as the external reference. Infrared spectra were recorded on a JASCO FT/IR-300E spectrometer. UV-visible spectra were recorded on a JASCO V-550 spectrometer. The content of Li was determined by ICP-AES (Shimadzu ICPS7510) after the sample treatment by a wet digestion method with concentrated nitric acid/30% H_2O_2 or only 30% H_2O_2. TGA spectra were obtained with a Shimadzu TA-50 instrument. Particle size was measured by the induced grating (IG) method (Shimadzu IG1000) for all samples and by scanning probe microscopy for Li@$C_{60}(OH)_{18}$. Zeta potentials were measured using a Malvern Instruments Zetasizer Nano ZSI instrument. SPM surface analysis was performed on a Shimadzu SPM-9700.

Synthesis of Li@$C_{60}(OH)_{18}$

The Li@C_{60} cluster was washed three times using *o*-dichlorobenzene and diethyl ether. The remaining insoluble material was used as the raw material for the synthesis (Li@C_{60}). To the starting material Li@C_{60} (50 mg), 60% fuming sulfuric acid (2.5 mL) was added, and the mixture was stirred for 24 h at 60 °C under an Ar atmosphere. After cooling to room temperature, the resulting mixture was dripped into chilled diethyl ether (100 mL). After centrifugation, the residual solid was washed three times with ca. 40 mL of diethyl ether, and dried under vacuum at 30 °C. The resulting reddish-brown solid was stirred in water (5 mL) for 60 h at 85 °C in air. After cooling to room temperature, the addition of a mixed solvent of 2-propanol, diethyl ether, and *n*-hexane (each 50 mL) gradually yielded a brown precipitate. After centrifugation, the residual solid was washed three times with ca. 40 mL of diethyl ether. Drying of the residue under a vacuum at 30 °C for 12 h resulted in Li@$C_{60}(OH)_{18}$·$6H_2O$ (54.4 mg, ca. 70%) as a brown powder. Elemental analysis: calc.

(100% Li@$C_{60}(OH)_{18}\cdot 6H_2O$) C: 63.12, H: 2.65, found C: 63.26, H: 2.35. Water content estimated by TGA, calc. 9.5%, found 9.5%. Quantitative analysis of lithium species by ICP-AES analysis: see below.

Synthesis of Reference $C_{60}(OH)_{16}$

To 60% fuming sulfuric acid (2.5 mL) was added C_{60} (50 mg), and the mixture was stirred for 16 h at 60 °C under an Ar atmosphere. After cooling to room temperature, the resulting mixture was dripped into chilled diethyl ether (100 mL). After centrifugation, the residual solid was washed three times with ca. 40 mL of diethyl ether, and dried under vacuum at 30 °C. The resulting reddish-brown solid was stirred in water (5 mL) for 30 h at 85 °C in air. After cooling to room temperature, the addition of a mixed solvent of 2-propanol, diethyl ether, and *n*-hexane (each 50 mL) gradually yielded a brown precipitate. After centrifugation, the residual solid was washed three times with ca. 40 mL of diethyl ether. Drying of the residue under a vacuum at 30 °C for 12 h resulted in $C_{60}(OH)_{16}\cdot 5H_2O$ (56.4 mg, 75%) as a brown powder. Elemental analysis: calc. C: 66.55, H: 2.42, found C: 67.29, H: 2.33. Water content estimated by TGA, calc. 8.3%, found 8.9%.

Quantitative Analysis of Lithium Species by ICP-AES

Before the measurement, 3.24 mg (ca. 2.84 μmol) of sample was completely degraded by heating it at 100 °C in 2 mL of concentrated nitric acid for 1 hour, followed by the addition of 30% hydrogen peroxide and further heating for 20 minutes, to release the Li^+ from the cage, and the resulting clear aqueous solution was then used for the analysis. The concentration of lithium in the sample was determined (0.100 ppm, 0.00250 mg/3.24 mg of sample, sum of internal and external Li^+), and the ratio of internal/external lithium cation was estimated by ^7Li NMR spectrum (92/8, 0.0023 mg (0.331 μmol)/0.0002 mg in 3.24 mg (2.84 μmol) of sample). Therefore, we calculated: 0.331/2.84 ×100 = 11.7 ≈ 12% of fullerenol molecules were lithium-encapsulated molecules.

Chapter 1-2. Hydroxylation of Purified [$Li^+@C_{60}$](PF_6^-)

1. Introduction

As mentioned above, various types of fullerenols have been reported; however, these fullerenols consist of a mixture of a wide variety of isomers with various numbers and positions of introduced hydroxyl groups, and only an average number of hydroxyl groups can be determined by elemental analysis except for recently synthesized $C_{60}(OH)_8$ as a single isomer.[9] Herein, the author wishes to report the unusual site-selective synthesis of Li-encapsulated fullerenol $Li^+@C_{60}O^-(OH)_7$ as a single major isomer along with two minor isomers when pure [$Li^+@C_{60}$](PF_6^-) was treated with fuming sulfuric acid. Although the regiochemical positions of hydroxyl groups could not be determined due to its C_1 symmetrical structure, its unique physicochemical properties based on both the internal Li^+ and the external –OH groups as well as the mechanistic aspects on site-selective hydroxylation were revealed.

2. Results and Discussion

The hydroxylation of [$Li^+@C_{60}$](PF_6^-) was carried out using the reported procedures under the optimized reaction conditions (Scheme 1).[3a] The product was characterized through infrared spectroscopy (IR), nuclear magnetic resonance spectroscopy (NMR), fast atom bombardment mass spectroscopy (FAB MS), thermogravimetric analysis (TGA) as well as the elemental analysis. The IR spectrum of the product is shown in Figure 1 along with that of the empty fullerenol $C_{60}(OH)_n$ (n = 10, as the average structure of a mixture of isomers) synthesized independently by the same fuming sulfuric acid method as a reference. The spectrum showed five characteristic bands at 3281,

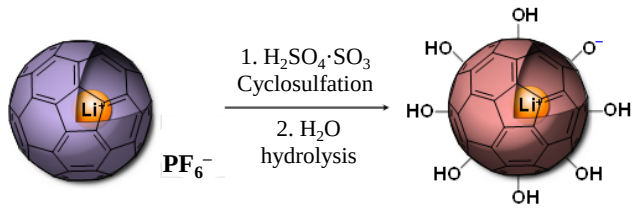

[$Li^+@C_{60}$](PF_6^-) $Li^+@C_{60}O^-(OH)_7$

Scheme 1. Synthesis of Li^+-encapsulated fullerenol.

1625, 1418, 1081, and 1040 cm^{-1} assignable to νO–H, νC=C, δ_sC–O–H and two types of νC–O, respectively. These absorption peaks clearly confirm the formation of fullerenol cage. Of interest is that the splitting of νC–O peak was observed only for Li^+ encapsulatedfullerenol. The higher energy band at 1080 cm^{-1} (by ca. 40 cm^{-1}) implies the appearance of the fullerenoxide C–O^- bond with enhanced bond order probably because of the deprotonation from one of the OH groups by electrostatic repulsion against the encapsulated Li^+ ion.[10]

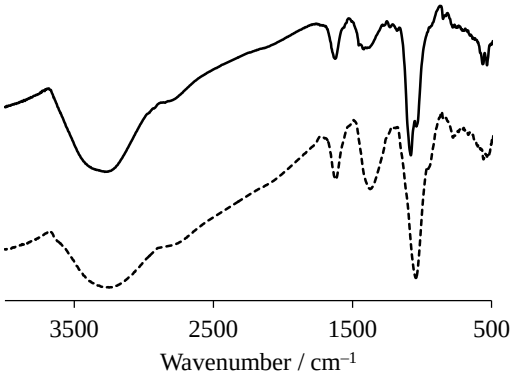

Compd.	Peaks / cm^{-1} (assigned to)			
Product	3281 (νO–H)	1625 (νC=C)	1418 (δ_sCOH)	1081, 1040 (νC–O)
$C_{60}(OH)_{10}$	3250	1622	1373	1044

Figure 1. IR spectra (KBr pellet method) of the product (solid) and empty fullerenol $C_{60}(OH)_{10}$ (dotted).

The encapsulated lithium cations were clearly detected by ^{7}Li NMR spectroscopy. In the spectrum obtained in DMSO-d_6, three characteristic signals were observed in the range of –15 to –19 ppm relative to LiCl in D_2O as an external standard (Figure 3). The observed upfield chemical shifts apparently suggest the encapsulation of Li^+ by π-conjugated fullerene cage. The abnormal higher upfield shift of the product than that of [Li^+@C_{60}]($SbCl_6^-$) salt (–10.5 ppm)[5] may be caused by the increased diamagnetic shielding effect of the appeared surface negative charge interacting with the inner lithium cation as mentioned above. These three sharp signals seem to correspond to a major

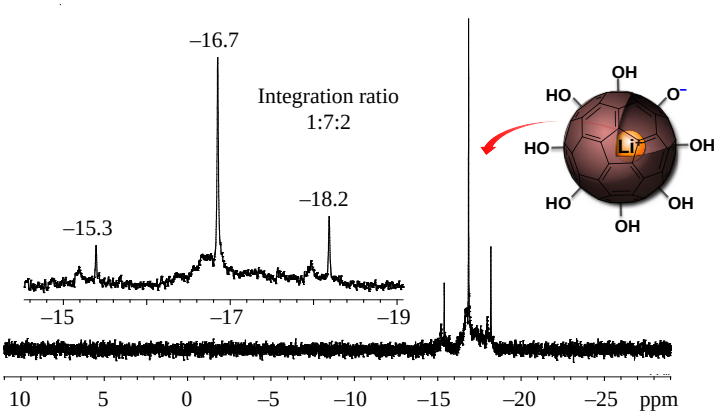

Figure 2. ^{7}Li NMR spectrum of the Li^+-encapsulated fullerenol in DMSO-d_6. The D_2O solution of LiCl was used as an external standard for the measurement of ^{7}Li NMR.

isomer (–16.7 ppm, ca. 70%) and two minor isomers (–15.3 and –18.2 ppm, ca. 10 and 20% by integration ratio), respectively. This ^{7}Li NMR spectrum is quite different from the highly broadened previous one which were observed on the measurement for Li@$C_{60}(OH)_{18}$ (*vide supra*), implying the formation of the less number of isomers possibly due to the unusual site-selective hydroxylation. Surprisingly, as shown in Figure 4, seven tall sharp peaks (*a*-*g*) along with four smaller minor peaks (*) assignable to –OH groups were clearly detected by ^{1}H NMR spectroscopy, whereas the empty fullerenol synthesized from pristine C_{60} showed a highly broadened signal centred at 7 ppm on account of the presence of a wide variety of isomers. These sharp peaks were found to disappear by addition of D_2O due to H/D exchange of the hydroxyl protons. The product distribution of isomers was also confirmed by HPLC analysis, consistent with ^{7}Li NMR (Figure 4). Whereas the three isomers could be detected clearly, their

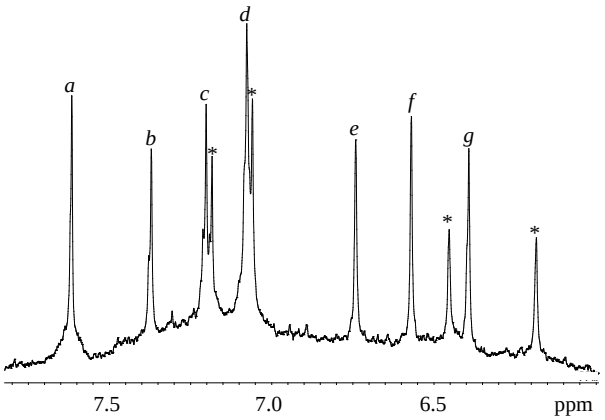

Figure 3. ^{1}H NMR spectrum of the Li^{+}-encapsulated fullerenol in DMSO-d_6.

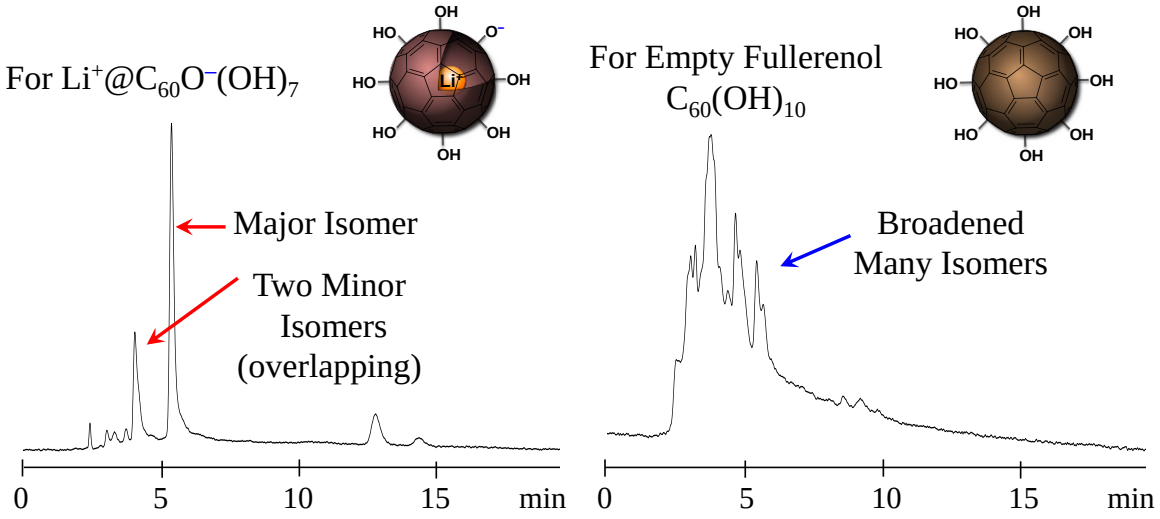

Figure 4. HPLC profiles of $Li^{+}@C_{60}O^{-}(OH)_7$ and empty $C_{60}(OH)_{10}$ analyzed using buckyprep (Nacalai Tesque COSMOSIL 4.6 × 250 nm) as a column, with DMF/methanol = 1/1 (v/v) in the presence of 0.1% TFA as an eluent at 40 ^{o}C.

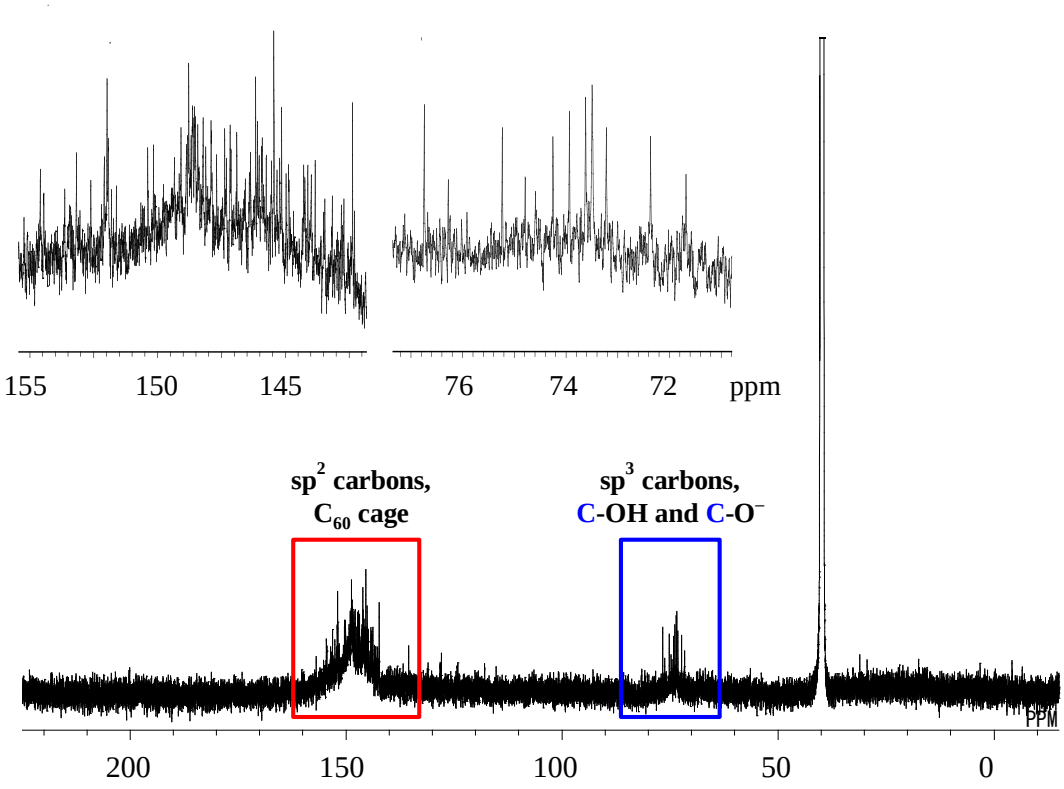

Figure 5. ^{13}C NMR spectra of the Li^+-encapsulated fullerenol in DMSO-d_6.

preparative separation was failed because 1) we could not secure enough amount of starting lithium encapsulated fullerene and 2) the product easily degraded during the separation process.

It was also noted that the ^{13}C NMR spectrum provided several signals assigned for sp^3 C–OH carbons at 72–77 ppm, probably eight large peaks and four small peaks, together with over 40 signals of sp^2 carbons at 140–160 ppm, in conformity with the C_1 symmetrical structure (Figure 5). Unfortunately, however, the peaks corresponding to the minor isomers could not be clearly observed due to the small amount of the sample even on 60,000 times accumulation.

Furthermore, we also confirmed the formation of lithium encapsulated fullerenol using positive mode fast atom bombardment mass spectroscopy (FAB MS) (Figure 6). The peaks at m/z = 863 was attributed to $Li^+@C_{60}O^-(OH)_7$, suggesting the encapsulation of lithium cation. The high resolution matrix-assisted laser desorption ionization time of flight (MALDI-TOF) mass spectroscopy also showed the molecular ion peak assignable to the same species. The UV-vis-NIR spectrum of the

product was essentially the same as that of the empty one. Finally, the structure was deduced from the elemental analysis as almost the same as the formula of $Li^+@C_{60}O^-(OH)_7 \cdot 4H_2O$ (Table 1).

From these findings, it is strongly indicated that the Li^+ encapsulated fullerenols consist of a single major regioisomer (ca. 70%) of $Li^+@C_{60}O^-(OH)_7$ which has seven OH groups and one fullerenoxide ($C_{60}O^-$) moiety with C_1 symmetry. As to the minor products it may be conceived of having a pair of 1) different regioisomers of the major one or 2) the more or less hydroxylated fullerenols.

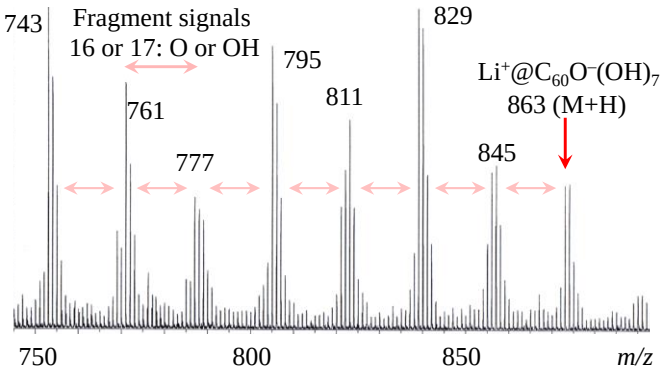

Figure 6. Positive mode FAB mass spectrum of the product. The peak observed at m/z = 863 attributed to $Li^+@C_{60}O^-(OH)_7$ ($M + H^+$) was detected. Other peaks at 743, 761, 777, 795, 811, 829, and 845 were fragment signals assignable to $Li^+@C_{60}O(OH)_{0-6}$, respectively.

Table 1. Elemental analysis of the product.

Average structure	Elemental analysis [%][a]	Water content [wt%][a,b]
Product	C: 77.16, H: 1.84	5.1
$Li@C_{60}O^-(OH)_7 \cdot 4H_2O$	(C: 77.10, H: 1.62)	(7.7)

[a] Values in parentheses are calculated data.
[b] Water content was determined by TGA.

Very interestingly, we confirmed that the counter anion PF_6^- was completely lost in the product on the basis of ^{31}P and ^{19}F NMR spectroscopy. This phenomenon can be explained by the formation of fullerenoxide ($C_{60}O^-$) anion moiety which no longer needs the counter anion such as PF_6^- (*vide supra*). The negative charge of fullerenoxide ($C_{60}O^-$) may be partly dispersed on the highly conjugated fullerene surface on account of the favourable electrostatic interaction with inner Li^+ ion. As the result, the Li^+ would highly be inclined toward one side of the inner wall of C_{60} as similarly reported in $[Li^+@C_{60}](SbCl_6^-)$, $[Li^+@PCBM](PF_6^-)$, and $[Li^+@C_{60}CpH](PF_6^-)$.[5,11,12] We have confirmed such Li^+ behavior by DFT calculation as mentioned above. Therefore, we propose the structure of $Li^+@C_{60}O^-(OH)_7$ without any free counter anion, and thus the compound could be

considered as "cation-encapsulated anion nanoparticle".

Why did the hydroxylation reaction of lithium encapsulated fullerene take place site-selectively? The time course of Vis-NIR spectra of the reaction intermediate in the cyclosulfation step recorded in fuming sulfuric acid $H_2SO_4 \cdot SO_3$ at room temperature provided telling clues about the reason.[3a] The spectrum just after the reaction started is shown in Figure 7 together with the case of empty C_{60} under the same conditions. The broad peak around 823 nm (dotted line) in the reaction of empty fullerene with fuming sulfuric acid suggests the generation of divalent cations of C_{60} (C_{60}^{2+}) through the two-electron oxidation which was induced by strong acceptor SO_3.[13] By contrast, the characteristic band of vis-NIR spectrum at 964 nm (solid line) and the ESR spectrum recorded in fuming sulfuric acid (Figure 8) for Li^+-encapsulated one indicated that the cation radical ($Li^+@C_{60}^{\bullet+}$) was exclusively produced through one-electron oxidation.[14] The lower *g* value (2.0016) compared with reported empty C_{60} radical cation and the line broadening was probably due to the polarity of fuming sulfuric acid and internal lithium cation.[15]

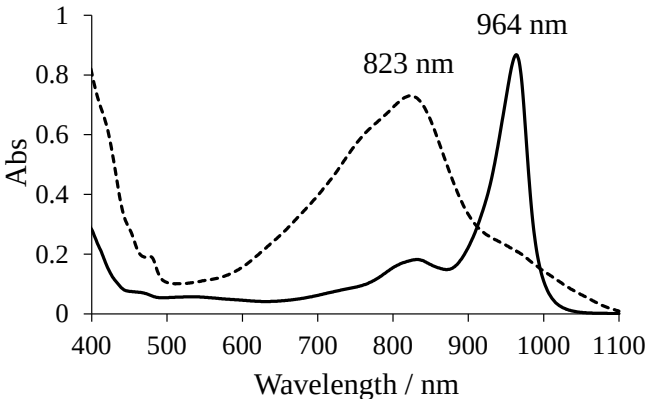

Figure 7. Vis-NIR spectra of the reaction intermediate during the cyclosulfation of $[Li^+@C_{60}](PF_6^-)$ (solid line) and empty fullerene (dotted line) in fuming sulfuric acid.

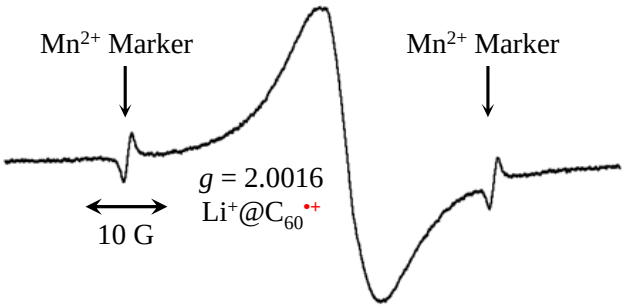

Figure 8. ESR spectrum of the reaction intermediate during the cyclosulfation of $[Li^+@C_{60}](PF_6^-)$ recorded in fuming sulfuric acid at 298 K calibrated by using a Mn^{2+}

These differences in the ionization potential between the Li^+ encapsulated C_{60} and the empty one can be rationalized by comparing their UV-vis spectra as well as the reduction potentials. The

UV-vis spectra of these fullerenes are almost superimposable, because of essentially the same HOMO-LUMO energy gaps. However, the first reduction potential, which corresponds to LUMO, of Li^+ encapsulated C_{60} was found to be 0.7 V more reducible than the empty one on cyclic voltammetry (CV) measurement. Therefore, the first oxidation potential which corresponds to HOMO should also be different by ca. 0.7 V due to the strong electron accepting ability of Li^+ and thus monovalent $Li^+@C_{60}^{\bullet+}$ seems to be sluggishly formed on fuming sulfuric acid oxidation, while the empty C_{60} can be easily oxidized to the divalent cation species.[13] Indeed, monovalent cation radical $Li^+@C_{60}^{\bullet+}$ was found to be persistent several days in fuming sulfuric acid, whereas divalent one degraded within several hours. Therefore, the cyclosulfation reaction of $[Li^+@C_{60}](PF_6^-)$ was quite slow as compared with the reaction of the empty one (Figure 9). This difference in the stability (i.e., reactivity) of the oxidized species is partly responsible for the difference in the site-selectivity of the multi-step addition of fuming sulfuric acid.[16] The vis-NIR spectrum of reaction intermediate of "$Li@C_{60}$ cluster" in fuming sulfuric acid was also measured as the comparison. However, no clear peak at ~960 nm which can be seen in the case of $[Li^+@C_{60}](PF_6^-)$ was observed probably due to the heterogeneous cluster nature of $Li^+@C_{60}^{-\bullet}$ surrounded by neutral C_{60} molecules. This electronic difference as well as the steric restriction could result in the unselective hydroxylation of $Li@C_{60}$ cluster.

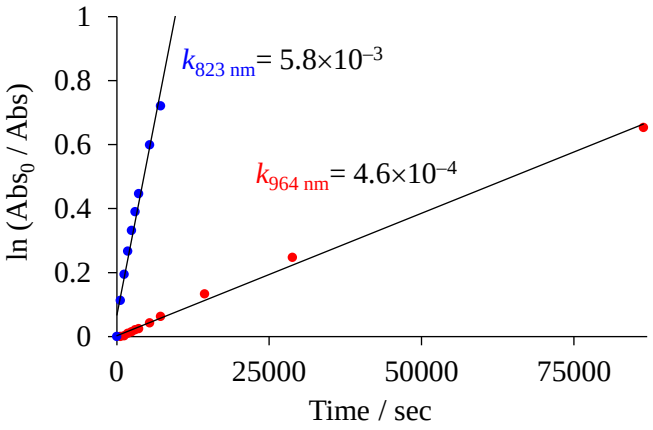

Figure 9. Ln plots of time course of NIR absorption change for the reaction of $[Li^+@C_{60}](PF_6^-)$ (red, 964 nm), empty C_{60} (blue, 823 nm) with fuming sulfuric acid at ambient temperature.

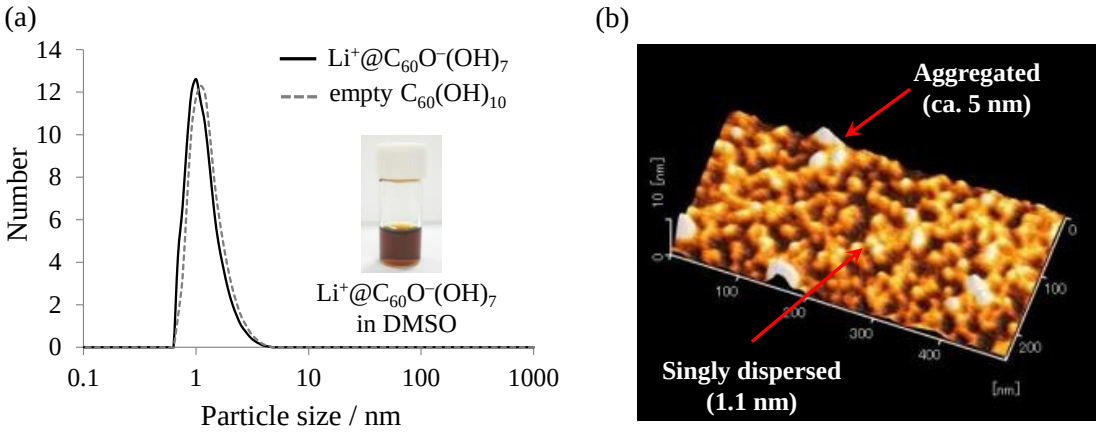

Figure 10. Particle size distribution of the product (black solid line) and reference fullerenol $C_{60}(OH)_{16}$ (gray dotted line) in DMSO analyzed by the induced grating method (a) and SPM particle analysis for the product (b).

One of the effects of the introduced hydroxyl groups to $[Li^+@C_{60}](PF_6^-)$ was the improvement of solubility. Although the low solubility of $[Li^+@C_{60}](PF_6^-)$ compared with pristine C_{60}, $Li^+@C_{60}O^-(OH)_7$ could be dissolved in polar solvent such as DMSO and DMF comparable with empty one. Indeed, the particle size analysis by induced grating (IG) method[8] showed the small and narrow particle size distribution (ca. 1.1 nm, original molecular size) in DMSO solution (Figure 10a). The size was also confirmed using scanning prove microscopy (SPM) for the sample prepared by applying the highly diluted aqueous solution of fullerenol to a mica plate and drying it (Figure 10b).

3. Conclusions

In summary, we synthesized $Li^+@C_{60}O^-(OH)_7$ using fuming sulfuric acid method from $[Li^+@C_{60}](PF_6^-)$ and characterized its structure by IR, NMR and FAB mass spectroscopy as well as the elemental analysis. Notably, the reaction of $[Li^+@C_{60}](PF_6^-)$ was site-selective to give a single major isomer (ca. 70%) with two minor isomers in marked contrast to the case of $Li@C_{60}$ cluster. We concluded from the analysis of radical species produced in the reaction of fuming sulfuric acid and C_{60} cage that this unusual site-selective hydroxylation was caused by the lower HOMO level of

lithium encapsulated fullerene than that of empty C_{60}. This result suggests the possibilities of the metal encapsulated fullerenes capable of becoming a new-type of fullerene multi-adducts with appreciable site-selectivity. Further mechanistic investigation on site-selectivity and the propertis of $Li@C_{60}^{\bullet+}$ are now undertaken as well as the application of our new Li^+ encapsulated fullerene compounds.

4. Experimental Section

General Procedure

$[Li^+@C_{60}](PF_6^-)$ was purchased from Idea International Corporation. All other reagents were commercially available and used without further purification. FAB mass spectrum and matrix assisted laser desorption ionization time-of-flight mass spectrum were measured on a JEOL JMS-700 and a Bruker autoflex III, respectively. The ^{7}Li, ^{1}H, ^{13}C and ^{19}F nuclear magnetic resonance (NMR) spectra were recorded at 233.12 MHz, 599.85 MHz, 150.84 MHz and 564.23 MHz on a Varian Unity Inova 600, respectively. ^{31}P NMR spectrum was recorded at 160.25 MHz on a JEOL ECS-400. Infrared spectra were recorded on a JASCO FT/IR-300E spectrometer. UV–visible-NIR spectra were recorded on a Shimadzu UV-1800 spectrometer. TGA spectra were obtained with a Shimadzu TA-50 instrument. ESR spectrum was measured on a JEOL JES-FA200. Particle size was measured by the induced grating (IG) method 10 (Shimadzu IG1000). SPM surface analysis was performed on a SII Nanonavi/Nanocute.

Synthesis of $Li^+@C_{60}O^-(OH)_7$

A slurry of $[Li^+@C_{60}](PF_6^-)$ (10 mg, 12 μmol) in 30% fuming sulphuric acid (0.5 mL) was stirred for 48 h at 60 °C under Ar atmosphere. After cooling to room temperature, the resulting mixture was dripped into chilled diethyl ether (100 mL). After centrifugation, the residual solid was washed three

times with ca. 10 mL of diethyl ether, and dried under vacuum at 30 °C. The resulting brown solid in water (3 mL) was stirred for 48 h at 70 °C under air. After cooling to room temperature, the suspension liquid was filtered off and the residual solid was washed with water until the solution was neutralized (40 mL). Then the solid was 20 washed three times with each ca. 40 mL of acetonitrile and diethyl ether. Drying of the residue under vacuum at 40 °C for 24 h resulted in $Li^+@C_{60}O^-(OH)_7 \cdot 4H_2O$ (9.2 mg, 9.9 μmol, 83%) as a brown powder.

Synthesis of Empty $C_{60}(OH)_{10}$

A slurry of C_{60} (36 mg, 50 μmol) in 30% fuming sulphuric acid (2.5 mL) was stirred for 48 h at 60 °C 25 under Ar atmosphere. After cooling to room temperature, the resulting mixture was dripped into chilled diethyl ether (200 mL). After centrifugation, the residual solid was washed three times with ca. 100 mL of diethyl ether, and dried under vacuum at 30 °C. The resulting brown solid in water (10 mL) was stirred for 30 h at 85 °C under air. After cooling to room temperature, the suspension liquid was filtered off and the residual solid was washed with water until the solution was neutralized (60 mL). Then the solid was 30 washed three times with each ca. 60 mL of acetonitrile and diethyl ether. Drying of the residue under vacuum at 40 °C for 24 h resulted in $C_{60}(OH)_{10} \cdot 4H_2O$ (42 mg, 44 μmol, 87%) as a brown powder.

References for Chapter 1

[1] (a) Chiang, L. Y.; Lu, F.-J.; Lin, J.-T. *J. Chem. Soc., Chem. Commun.* **1995**, 1283. (b) Kato, S.; Aoshima, H.; Saitoh, Y.; Miwa, N. *Bioorg. Med. Chem. Lett.* **2009**, *19*, 5293. (c) Xiao, L.; Aoshima, H.; Saitoh, Y.; Miwa, N. *Free Radic. Biol. Med.* **2011**, *51*, 1376.

[2] Sardenberg, R. B.; Teixeira, C. E.; Pinheiro, M.; Figueiredo, J. M. A. *ACS Nano* **2011**, *5*, 2681.

[3] (a) Chiang, L. Y.; Wang, L. -Y.; Swirczewski, J. W.; Soled, S.; Cameron, S. *J. Org. Chem*. **1994**,

59, 3960–3968. (b) Chiang, L. Y.; Upasani, R. B.; Swirczewski, J. W. *J. Am. Chem. Soc*. **1992**, *114*, 10154. (c) Chiang, L. Y.; Swirczewski, J. W.; Hsu, C. S.; Chowdhury, S. K.; Cameron, S.; Creegan, K. *J. Chem. Soc., Chem. Commun*. **1992**, 1791. (d) Chiang, L. Y.; Bhonsle, J. B.; Wang, L.; Shu, S. F.; Chang, T. M.; Hwu, J. R. *Tetrahedron* **1996**, *52*, 4963. (e) Schneader, N. S.; Darwish, A. D.; Kroto, H. W.; Taylor, R.; Walton, D. R. M. *J. Chem. Soc., Chem. Commun*. **1994**, 463. (f) Wang, S.; He, P.; Zhang, J.-M.; Jiang, H.; Zhu, S.-Z. *Synth. Commun*. **2005**, *35*, 1803. (g) Arrais, A.; Diana, E. *Fuller. Nanotub. Carbon Nanostruct*. **2003**, *11*, 35. (h) Li, J.; Takeuchi, A.; Ozawa, M.; Li, X.; Saigo, K.; Kitazawa, K. *J. Chem. Soc., Chem. Commun*. **1993**, 1784. (i) Kokubo, K.; Matsubayashi, K.; Tategaki, H.; Takada, H.; Oshima, T. *ACS Nano* **2008**, *2*, 327. (j) Kokubo, K.; Shirakawa, S.; Kobayashi, N.; Aoshima, H.; Oshima, T. *Nano Res*. **2011**, *4*, 204.

[4] (a) Mikawa, M.; Kato, H.; Okumura, M.; Narazaki, M.; Kanazawa, Y.; Miwa, N.; Shinohara, H. *Bioconjugate Chem*. **2001**, *12*, 510. (b) Sitharaman, B.; Bolskar, R. B.; Rusakova, I.; Wilson, L. J. *Nano Lett*. **2004**, *4*, 2373.

[5] Aoyagi, S.; Nishibori, E.; Sawa, H.; Sugimoto, K.; Takata, M.; Miyata, Y.; Kitaura, R.; Shinohara, H.; Okada, H.; Sakai, T.; Ono, Y.; Kawachi, K.; Yokoo, K.; Ono, S.; Omote, K.; Kasama, Y.; Ishikawa, S.; Komuro, T.; Tobita, H. *Nat. Chem*. **2010**, *2*, 678.

[6] Popok, V. N.; Azarko, I. I.; Gromov, A. V.; Jönsson, M.; Lassensson, A.; Campbell, E. E. B. *Solid State Commun.* **2005**, *133*, 499.

[7] Husebo, L. O.; Sitharaman, B.; Furukawa, K.; Kato, T.; Wilson, L. Fullerenols Revisited as Stable Radical Anions. J. *J. Am. Chem. Soc.* **2004**, *126*, 12055.

[8] Wada, Y.; Totoki, S.; Watanabe, M.; Moriya, N.; Tsunazawa, Y.; Shimaoka, H. *Optics Express* **2006**, *14*, 5755.

[9] Zhang, G.; Liu, Y.; Liang, D.; Gan, L.; Li, Y. *Angew. Chem. Int. Ed*. **2010**, *49*, 5293.

[10] Seubold, R. H. Jr *J. Org. Chem.* **1956**, *21*, 156.

[11] Matsuo, Y.; Okada, H.; Maruyama, M.; Sato, H.; Tobita, H.; Ono, Y.; Omote, K.; Kawachi, K.;

Kasama, Y. *Org. Lett.* **2012**, *14*, 3784.

[12] Kawakami, Y.; Okada, H.; Matsuo, Y. *Org. Lett*. **2013**, 15, 4466.

[13] (a) Thomann, H.; Bernardo, M.; Miller, G. P. *J. Am. Chem. Soc.* **1992**, *114*, 6593. (b) Cataldo, F. *Spectrochim. Acta* **1995**, *51A*, 405. (c) Solodovnikov, S. P. *Russ. Chem. Bull.* **1998**, *47*, 2302.

[14] Webster, R. D.; Heath, G. A. *Phys. Chem. Chem. Phys*. **2001**, *3*, 2588.

[15] (a) Kukolich, S. G.; Huffman, D. R. *Chem. Phys. Lett.* **1991**, *182*, 263. (b) Fukuzumi, S.; Suenobu, T.; Urano, T.; Tanaka, K. *Chem. Lett.* **1997**, 875. (c) Tanaka, K.; Ago, H.; Matsuura, Y.; Kuga, T.; Yamabe, T.; Yuda, S.; Hato, Y.; Ando, N. *Synth. Met.* **1997**, *89*, 133.

[16] (a) Johnson, C. D. *Chem. Rev.* **1975**, *75*, 755. (b) Giese, B. *Angew. Chem, Int. Ed. Engl.* **1977**, *16*, 125. (c) Pross, A. in Advances in Physical Organic Chemistry, ed. Gold, V. and Bethell, D. Academic Press, London, New York, San Francisco, 1977, vol. 14, p. 69

Chapter 2:

Kinetic Study in Diels-Alder Reaction of $Li^+@C_{60}$ with 1,3-Cyclohexadiene

Diels-Alder reaction is the most studied functionalization procedure for fullerenes. The [6,6] double bonds on fullerene cage are excellent dienophiles because of the lower lying LUMO as compared with various olefins. Considering the strong electron acceptability of Li^+-encapsulated fullerene, it may react with a lot of reagents which cannot act as nucleophile for empty and other endohedral fullerenes. It is no doubt that the precise examination of the reactivity is the fundamental study to develop the $Li^+@C_{60}$ chemstry. In chapter 2, the author wishes to present about Diels-Alder product of $Li^+@C_{60}$ with 1,3-cyclohexadiene coupled with the kinetic experiment of the reaction.

1. Introduction

As mentioned above, based on the notably enhanced electron acceptability and ionicity of $Li^+@C_{60}$, several studies on $Li^+@C_{60}$ concerning the photo-induced electron transfer and its unique ionic nature have been reported.[1,2] For the tuning of peculiar physic-chemical properties of the novel endohedral fullerene, the chemical functionalization can be a powerful tool to provide some unique properties to the fullerenes as have been studied in our group since the first report of $Li^+@C_{60}$. Although some Li^+-encapsulated fullerene derivatives have been reported including above mentioned multihydroxylated derivatives,[3] the study on the reactivity of $Li^+@C_{60}$ was relatively stagnant as compared with the empty fullerenes.[4] It is no doubt that development of optimized synthetic technique and precise kinetic study of the reactivity will play an important role for the new application of $Li^+@C_{60}$. Herein the author reports the synthesis of $Li^+@C_{60}(C_6H_8)$ by Diels-Alder (DA) reaction and characterization of the product as well as the kinetic evaluation of the enhanced reactivity of $Li^+@C_{60}$.

2. Results and Discussion

The 1,3-cyclohexadiene (C_6H_8) was chosen for our kinetic examination in DA reaction because it has the simple structure and the suitable reactivity for the measurement on both C_{60} and $Li^+@C_{60}$. In our experiments, the second-order rate constants in DA reaction of empty C_{60} with 1,3-dienes widely distributed in the range of 10^5k_2 = 1.8–17000 $M^{-1}s^{-1}$ at 303 K (Table 1). The synthesis was carried out according to Scheme 1 under dark condition. The reaction progress was monitored using the reported electrolyte-containing HPLC technique, and the desired monoadduct was isolated by a preparative HPLC method (see experimental section). The product was characterized through $^1H/^{13}C/^7Li$ NMR, atmospheric pressure chemical ionization time of flight (APCI-TOF) mass spectroscopy as well as single-crystal X-ray structural analysis. The ^1H and ^{13}C NMR spectra of the product was quite similar to those of empty $C_{60}(C_6H_8)$ and revealed the same *C*s-symmetrical structure with the reported [6,6]-monoadduct.[5] The ^7Li NMR spectrum showed a sharp signal at –13.5 ppm which was slightly upper field as compared with the starting $[Li^+@C_{60}](PF_6^-)$,[6] indicating that the Li^+ surely existed in the highly shielded fullerene cage. The high resolution APCI-TOF mass spectrum also revealed the formation of the desirable monoaduct with a signal at 807.0773 assignable to the molecular ion (M^+, calcd 807.0786). Finally, the structure was confirmed by X-ray structural analysis after exchanging the counter anion from

Table 1. Second-order rate constants k_2 for the reaction of 1,3-dienes with empty C_{60} at 303 K in toluene.

1,3-dienes	10^5k_2 / $M^{-1}s^{-1}$
cyclopentadiene	17000
9-methylanthracene	2620
2-methyl-1,3-pentadiene	50.7
anthracene	26.7
2,3-dimethyl-1,3-butadiene	7.70
1,3-cyclohexadiene	**6.71**
2-methyl-1,3-butadiene	3.02
1,4-diphenyl-1,3-butadiene	2.12
2,3-dimethoxy-1,3-butadiene	1.89

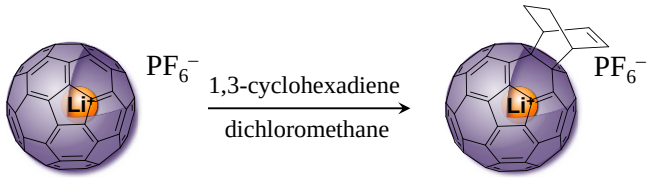

$[Li^+@C_{60}](PF_6^-)$ $[Li^+@C_{60}(C_6H_8)](PF_6^-)$

Scheme 1. DA reaction of $[Li^+@C_{60}](PF_6^-)$ with 1,3-cyclohexadiene. (10 equiv. for preparation and 100 equiv. for kinetic measurement.

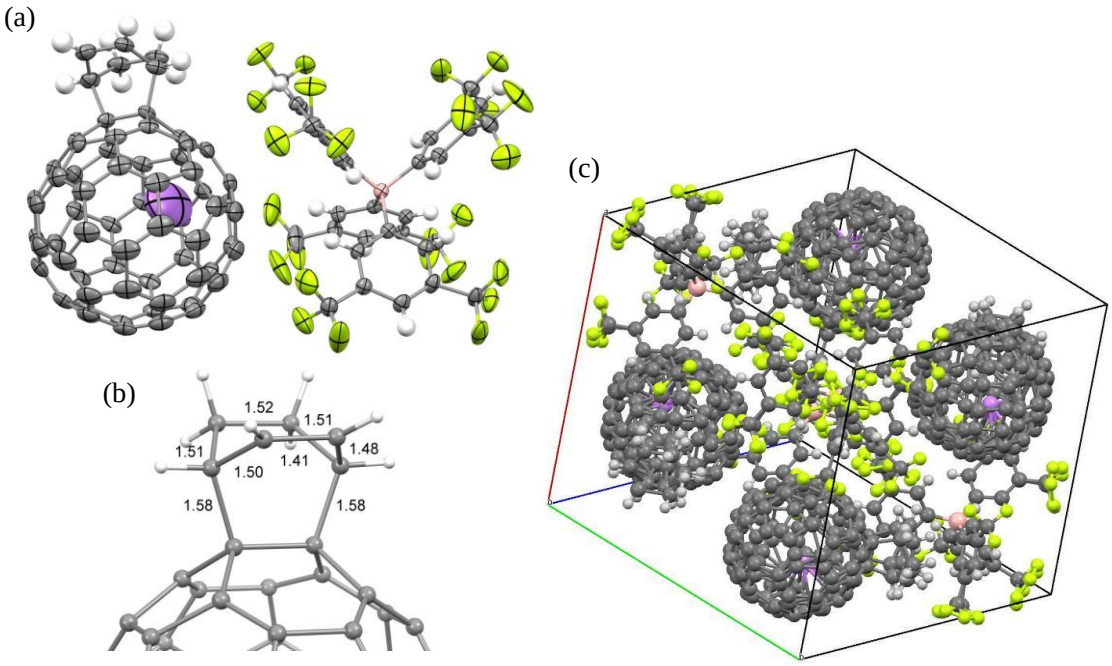

Figure 1. Crystal structure of $[Li^+@C_{60}(C_6H_8)]TFPB^-$: (a) anion/cation pair in the crystal; (b) C_6H_8 moiety on the fullerene cage; (c) packing structure. The C-C bond lengths in angstrom unit are also shown in the figure.

PF_6^- to tetrakis[3,5-bis(trifluoromethyl)phenyl]borate ($TFPB^-$, $B[C_6H_3(CF_3)_2]^-$ by our reported procedure as shown in Figure 1.[7] The crystal structure showed that the addition of C_6H_8 to C_{60} cage occurred at the (6,6)-bond, in good agreement with the results of quantum mechanical studies.[8] The encapsulated Li^+ was located near the 6-membered ring which interacted with one of the $C_6H_3(CF_3)_2$ moieties of TFPB counter anion. The obtained $[Li^+@C_{60}(C_6H_8)](PF_6^-)$ was very stable in solution, and the retro DA reaction and any decomposition did not occur even if the solution was heated at 373 K over 24 hours, because $Li^+@C_{60}$-based DA products are much more stable than the corresponding empty DA derivatives due to the lager interaction by lower-lying LUMO of $Li^+@C_{60}$ with HOMO of C_6H_8 (*vide infra*).[9]

In this synthesis, the author had to be careful with "photo-irradiation" to avoid generation of byproduct. The author supposed that the other product observed in ^7Li NMR spectrum at –13.3 ppm was produced by photo [2+2] reaction of $[Li^+@C_{60}](PF_6^-)$ and 1,3-cyclohexadiene as shown in Figure 2a. The signal at –13.3 ppm was slightly observed in the case of dark condition (Figure 2b).

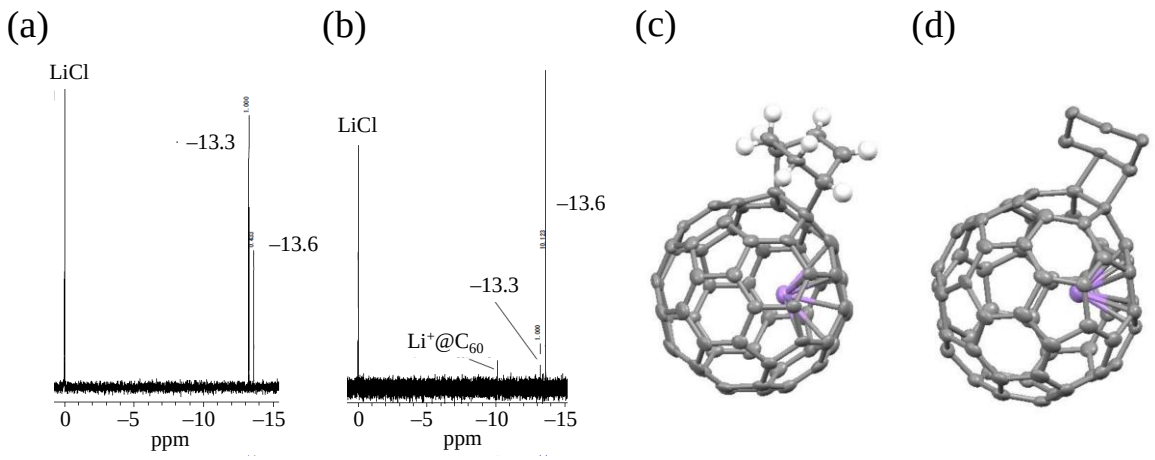

Figure 2. ^{7}Li NMR spectra of the crude products synthesized (a) under photo-irradiated condition and (b) under dark, and X-ray structure of [4+2] (c) and [2+2] (d) adducts obtained from co-crystal of the crude product synthesized under photo-irradiation condition.

Considering the 0.7 eV lower-lying LUMO level of $Li^{+}@C_{60}$ relative to empty C_{60}, photo-induced electron transfer from cyclohexadiene to $Li^{+}@C_{60}$ might give the photo [2+2] cycloadduct.[10] The result of X-ray structural analysis for the co-crystal is shown in Figure 2c, indicating the generation of [2+2] product. In previous study on the Diels-Alder reaction of $Li^{+}@C_{60}$ with cyclopentadiene, the similar phenomenon was not observed because of the more distant energy level of cyclopentadiene for $Li^{+}@C_{60}$. Further isolation and characterization of the photo product were now under progress.

The kinetic measurements for the DA reaction were performed under pseudo-first-order conditions, using a large excess of C_6H_8 (100 eq) at 253, 263, and 273 K for $Li^{+}@C_{60}$ in dichloromethane (CH_2Cl_2) and at 353, 363, and 373 K for empty C_{60} in

Table 2. Second-order rate constants k_2 for the reaction of 1,3-dienes with empty C_{60} at 303 K in toluene.

Solvents	$10^5 k_2$ / $M^{-1}s^{-1}$
beozonitrile	22.6
1-methylnaphthalene	14.9
bromobenzene	14.7
***o*-dichlorobenzene**	14.1
anisole	13.7
chlorobenzene	13.3
benzene	12.1
dichloromethane	10.3
tetralin	9.74
carbon disulfide	8.95
tetrachloromethane	8.68
chloroform	7.91
hexane	7.77
p-xylene	7.47
toluene	6.71
mesitylene	5.74

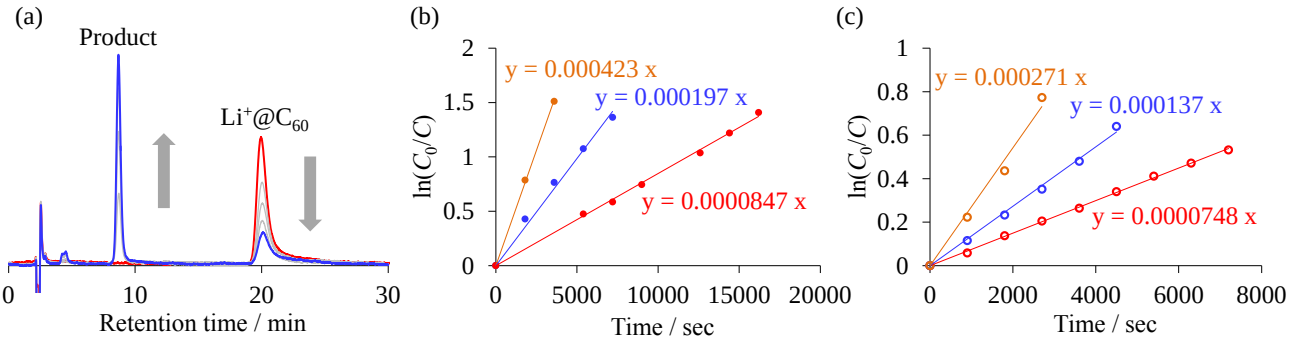

Figure 3. (a) Representative HPLC profile of the DA reaction of $[Li^+@C_{60}](PF_6^-)$ with 1,3-cyclohexadiene in CH_2Cl_2 at 263 K in dark. Plots of $\ln(C_0/C)$ vs time in the DA reaction of (b) $[Li^+@C_{60}](PF_6^-)$ and (c) empty C_{60} with 1,3-cyclohexadiene. The pseudo-first-order rate constants of the reaction are obtained from the slopes. The C_0 and C are an initial concentration and the concentration at the time of fullerene, respectively.

o-dichlorobenzene (*o*-DCB), respectively. Whereas the different solvents were used due to the temperature limitation, we confirmed that no remarkable difference in kinetic behavior was observed between these solvents on the kinetic measurements of empty C_{60} (Table 2). The progress of the reaction was followed by HPLC, using a Buckyprep column. The representative HPLC chart obtained for the kinetic solution is shown in Figure 3a. The second-order rate constants k_2 were obtained from the measured pseudo-first-order rate constants k' according to the Figure 3b, 3c, and the following equation (1).

$$-d[Li^+@C_{60}]/dt = k'[Li^+@C_{60}] = k_2[Li^+@C_{60}][C_6H_8] \quad (1)$$

These k_2 at various temperatures are listed in Table 3 along with the estimated k_2 values at 303 K by extrapolation in Arrhenius plot (see below). The ratio of k_2 ($Li^+@C_{60}$ vs C_{60} at 303 K) revealed that DA reaction of $[Li^+@C_{60}](PF_6^-)$ was ca. 2400 times accelerated relative to the reaction of empty C_{60} by the encapsulated Li^+.

Table 3. Second-order rate constants in the DA reaction of $[Li^+@C_{60}](PF_6^-)$ and empty C_{60} with C_6H_8.

$[Li^+@C_{60}](PF_6^-)$		empty C_{60}	
Temp. / K	10^5k_2 / $M^{-1}s^{-1}$	Temp. / K	10^5k_2 / $M^{-1}s^{-1}$
253	1344	353	1187
263	3129	363	2167
273	6714	373	4302
303	52300[a)]	303	21.3[a)]

a) Estimated by extrapolation in Arrhenius plot.

Based on the results, activation parameters, such as activation energy E_a, activation enthalpy $\Delta H^{\ddagger}$, activation entropy $\Delta S^{\ddagger}$, and

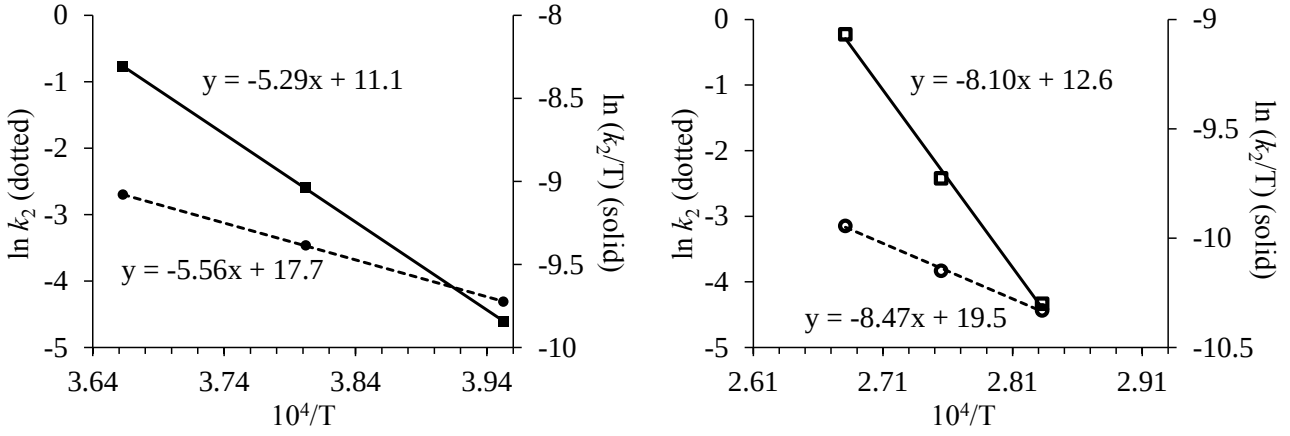

Figure 4. Arrhenius plots (dotted) and Eyring plots (solid) in the DA reaction of $[Li^+@C_{60}](PF_6^-)$ (left) and empty C_{60} (right) with 1,3-cyclohexadiene.

activation Gibbs free energy $\Delta G^{\ddagger}$, were obtained by Arrhenius plot ($\ln k_2$ vs 1/T) and Eyring plot ($\ln(k_2/T)$ vs 1/T) (Figure 4) according to the following Arrhenius equation:[11]

$$\ln k_2 = -E_a/RT + \ln A \qquad (2)$$

Here, $\ln A$ is a constant. The eqn. (2) leads the following eqn. (3):

$$\ln (k_2/T) = -\Delta H^{\ddagger}/RT + [\ln (\kappa k_B/h) + \Delta S^{\ddagger}/R] \qquad (3)$$

Here, κ is the permeation constant which is approximately 1 in our system. The k_B and h are the Boltzmann constant and the Plank constant, respectively. The E_a in the DA reaction of $Li^+@C_{60}$ with C_6H_8 (46.2 kJ mol^{-1}) was ca. 24 kJ/mol lower than that of empty C_{60} (70.4 kJ mol^{-1}). This is probably because of the stabilization of the partial polarization in transition state caused by the electrostatic field of encapsulated Li^+ in addition to the increased HOMO–LUMO interaction due to the lower LUMO level of $Li^+@C_{60}$. It is well known that Lewis acids accelerate some DA reactions,[12] and thus the observed rate enhancement can be recognized as the similar effect by the encapsulated Li^+. In general, the rate constant of DA reaction is mainly dominated by not only the energy difference between HOMO of the diene and LUMO of the dienophile, but also the steric configuration of each π-orbital of diene and dienophile.[4] In our experiment, because $Li^+@C_{60}$ and empty C_{60} have essentially the same [60]fullerene core, the steric effect did not affect to the kinetic

behavior. Thus, in a certain reaction like DA reaction, the encapsulated Li^+ can act as an *intramolecular reaction mediator*.

The enhancement of the reactivity in the DA reaction was well consisted with the results of DFT calculation as shown in Figure 5. The calculated energy difference between each substrate and transition state indicated that the activation energy in the reaction of $Li^+@C_{60}$ was lower than that of empty C_{60} and there is a good correlation between experimentally obtained values and calculated one. It is noteworthy that the optimized transition state in the DA reaction of $Li^+@C_{60}$ showed asymmetrical approach of cyclohexadiene to the fullerenyl cage without regard for the almost symmetrically expanded LUMO of $Li^+@C_{60}$. This result indicates that the reaction mechanism in DA reaction of $Li^+@C_{60}$ with C_6H_8 has stepwise nature in part probably due to the more polarized transition state and the partial charge transfer from C_6H_8 to $Li^+@C_{60}$, which is different from the common concerted mechanism in the DA reaction of empty C_{60}. Furthermore, the calculated energy difference between the substrates and the products suggested the further stabilization of $Li^+@C_{60}(C_6H_8)$, being explained by the energy gained in orbital interaction ΔE according to

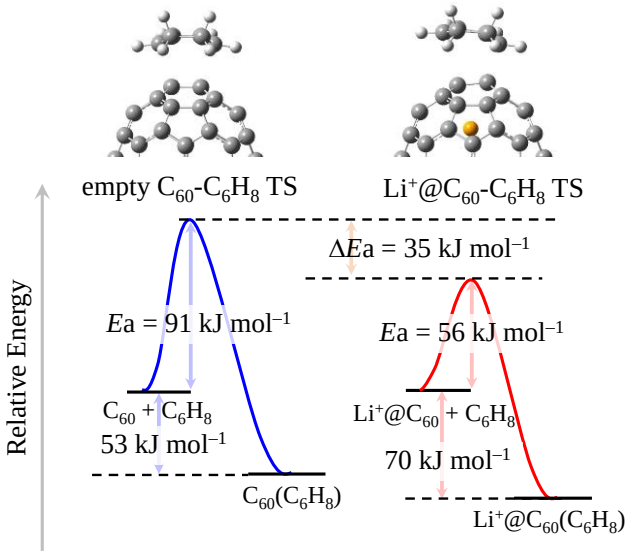

Figure 5. Relative energy changes in the DA reaction of empty C_{60} (left) and $Li^+@C_{60}$ (right) with C_6H_8 estimated by DFT calculation (B3LYP/6-31G*).

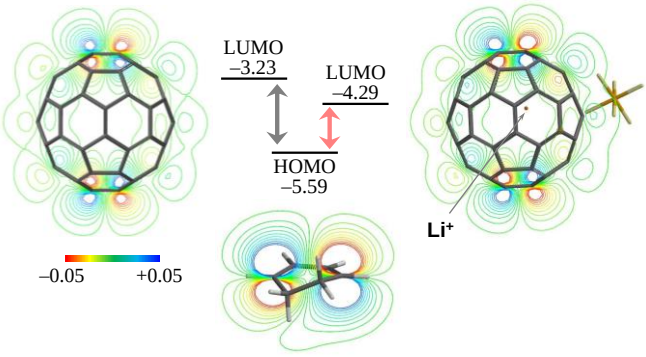

Figure 6. Calculated LUMO energies of $Li^+@C_{60}$, empty C_{60} and HOMO energy of C_6H_8 (eV) by B3LYP/6-31G* method.

Klopman and Salem equation (4):[13]

$$\Delta E = 2(C_a C_b \beta_{ab})^2/|e_a - e_b| = \text{constant} \times (C_a C_b)^2/|e_a - e_b| \qquad (4)$$

The C_aC_b denote the overlap of MO coefficients of interacting atomic orbitals. The term β_{ab} is the resonance integral that converts the efficiency of overlap to the energy units. LUMO energies (e_a) of fullerenes and HOMO energy (e_b) of C_6H_8 were calculated by B3LYP/6-31G* level and shown in Figure 6 along with their schematic images. Because $Li^+@C_{60}$ has lower LUMO level (closer to HOMO of C_6H_8) than empty C_{60} and thus the term $|e_a - e_b|$ is smaller in the reaction of $Li^+@C_{60}$ as compared with empty C_{60}, the ΔE becomes larger to give more stabilized $Li^+@C_{60}(C_6H_8)$ as depicted in Figure 5.

3. Conclusions

In summary, the author synthesized and characterized new Li^+-encapsulated fullerene derivative $[Li^+@C_{60}(C_6H_8)](PF_6^-)$ by Diels-Alder reaction of $[Li^+@C_{60}](PF_6^-)$ with C_6H_8. The kinetic study revealed that the reaction was ca. 2400 times faster than that of empty C_{60} because of the increased interaction by the lower-lying LUMO of $Li^+@C_{60}$ with the HOMO level of C_6H_8. The remarkable rate enhancement was rationalized by 24 $kJmol^{-1}$ smaller activation energy which was estimated by Arrhenius and Eyring plots as well as other kinetic parameters such as $\Delta H^{\ddagger}$, $\Delta S^{\ddagger}$, and $\Delta G^{\ddagger}$. All these results were caused by the encapsulated lithium cation, considering the reaction as "encapsulated Li^+-mediated" DA reaction.

4. Experimental Section

General Procedure

$[Li^+@C_{60}](PF_6^-)$ was obtained from Idea International Corporation. All other reagents were commercially available and used without further purification. High resolution mass spectra were obtained by APCI using a time-of-flight mass analyzer on JEOL JMS-T100LC (AccuTOF)

spectrometer with a calibration standard of polyethylene glycol (MW 1000). The ^{7}Li, ^{1}H, and ^{13}C NMR spectra were recorded at 233.12 MHz, 599.85 MHz and 150.84 MHz on a Varian Unity Inova 600. UV-visible spectrum was recorded on a Simadzu UV-1800 spectrometer.

Synthesis of $[Li^{+}@C_{60}(C_6H_8)](PF_6^{-})$

1,3-Cyclohexadiene (dichloromethane solution, 53.7 mM, 2 mL, 107 μmol) was slowly added to a dichloromethane solution (47 mL) of $[Li^{+}@C_{60}]PF_6^{-}$ (9.37 mg, 10.7 μmol) and reacted at 273 K for 150 min. Then unreacted 1,3-cyclohexadiene was removed in *vacuo* after dilution of the crude solution by adding chlorobenzene (30 mL) to avoid further reaction progress in this process. Purification of the product was performed with electrolyte–added HPLC using πNAP (Nacalai Tesque COSMOSIL 4.6 × 250 nm) as a column, with chlorobenzene: 1,2-dichloroethane:acetonitrile = 2:1.5:6.5 (v/v/v) in the presence of saturated Me_4NPF_6 as an eluent at 303 K. After evaporating the solvent in *vacuo*, dichloromethane was added to the red-brown residue containing white solids of Me_4NPF_6. After removing the solid by filtration, recrystallization from the solution by vapor-diffusion with diethyl ether at 273 K gave brown crystals of $[Li^{+}@C_{60}(C_8H_6)]PF_6^{-}$ (1.8 mg, 18 %, 1.9 μmol, red-brown solid). ^{1}H NMR (600 MHz, dichloromethane-d_2): δ 7.34 (dd, J = 3.2 Hz, 2H, vinyl H_D), 4.26 (m, 2H, bridgehead H_C), 3.10 (m, 2H, H_A or H_B), 2.31 (m, 2H, H_A or H_B). ^{13}C NMR (151 MHz, dichloromethane-d_2): δ 156.88 (s), 156.24 (s), 146.46 (s), 145.54 (s), 145.46 (s), 145.31 (s), 145.28 (s), 145.16 (s), 144.81 (s), 144.49 (s), 144.47 (s), 144.35 (s), 144.07 (s), 143.54 (s), 143.29 (s), 142.43 (s), 142.07 (s), 141.92 (s), 141.07 (s), 140.78 (s), 140.77 (s), 140.68 (s), 140.63 (s), 140.57 (s), 139.00 (s), 138.94 (s), 136.38 (s), 135.40 (s), 135.14 (s), 70.48 (s), 42.87 (s), 24.59 (s). ^{7}Li NMR (233 MHz, dichloromethane-d_2): δ –13.5 (s). High-resolution APCI-TOF MS (+): m/z calcd. for $C_{66}H_8Li$, 807.0786; found, 807.0773.

X-ray Structural Analysis of $[Li^+@C_{60}(C_6H_8)]TFPB^-$.

Structural characterization of $Li^+@C_{60}(C_6H_8)$ was performed by means of single crystal X-ray diffraction of $[Li^+@C_{60}(C_6H_8)]TFPB^-$. $[Li^+@C_{60}(C_6H_8)]PF_6^-$ (0.2 mg) and LiTFPB (1.1 mg, excess) were dissolved in 4 mL of dichloromethane with ultrasonic agitation (1 min). Then, the solution was filtered and concentrated in *vacuo* to ~60 mL. Recrystallization from the solution by vapor-diffusion with diethyl ether at 273 K gave brown crystals of $[Li^+@C_{60}(C_6H_8)]TFPB^-$. The synchrotron-radiation X-ray diffraction measurement was performed by using the large cylindrical image-plate camera at SPring-8 BL02B1 (Hyogo, Japan) at 150 K. The crystal structure analysis was performed by using *SHELX*. The results are summarized in Table S1. The $Li^+@C_{60}(C_6H_8)$ molecule has a disordered structure with two molecular orientations. The two molecular orientations evenly coexist in the crystal. The encapsulated Li^+ cation is localized under a six-membered ring so that the C_s symmetry of the molecule brakes in the crystal.

Table S1. Crystallographic Data for $[Li^+@C_{60}(C_6H_8)]TFPB^-$.

formula	$[LiC_{60}(C_6H_8)]B((CF_3)_2C_6H_3)_4$
formula weight	1670.89
color of crystal	Black
temperature	150 K
X-ray wavelength	0.64898 Å
crystal system	Monoclinic
space group	$P\ 2_1/n$
unit cell parameters	a = 17.5861(4) Å
	b = 19.0753(4) Å
	c = 19.3177(8) Å
	b = 92.707(3) °
Z	4
No. of independent reflections	15,394 (d > 0.63 Å, $\|F\| > 2s$)
Ss_I/SI	0.044
No. of parameters	1,478
$R1$	0.0581 ($\|F\| > 2s$)
GOF	0.854 ($\|F\| > 2s$)

The Kinetic Evaluation in the Diels-Alder Reaction of [Li^+@C_{60}](PF_6^-) and Empty C_{60} with 1,3-cyclohexadiene (and other 1,3-dienes)

The kinetic measurements for the DA reaction of [Li^+@C_{60}](PF_6^-) and empty C_{60} with 1,3-cyclohexadiene were performed under pseudo-first-order conditions by using a large excess amount of diene (ca. 100 eq, 6 mM) relative to fullerenes (ca. 60 μM) under dark. The progress of the reaction was followed by monitoring the consumption of C_{60} with HPLC; For [Li^+@C_{60}](PF_6^-); column: Buckyprep (Nacalai Tesque COSMOSIL 4.6 × 250 nm), eluent: *o*-dichlorobenzene:acetonitrile = 9:1 (v/v) with saturated $^nBu_4NPF_6$, temperature: RT. ; For empty C_{60}; column: Buckyprep (Nacalai Tesque COSMOSIL 4.6 × 250 nm), eluent: toluene, temperature: RT. Monitoring the kinetic reaction by HPLC showed the gradual increase of monoadduct ([Li^+@C_{60}(C_6H_8)](PF_6^-) or empty C_{60}(C_6H_8)) accompanied by the decay of starting material. The natural logarithmic plots of the signal intensities of the remaining starting fullerenes relative to those of the first aliquots (t = 0) gave the linear correlation. The obtained slope, that is, the pseudo-first-order rate constant k', was divided by the concentration of 1,3-cyclohexadiene to provide the second-order rate constants k_2.

References for Chapter 2

[1] Fukuzumi, S.; Ohkubo, K.; Kawashima, Y.; Kim, D. S.; Park, J. S.; Jana, A.; Lynch, V. M.; Kim, D.; Sessler, J. L. *J. Am. Chem. Soc.* **2011**, *133*, 15938.

[2] Aoyagi, S.; Sado, Y.; Nishibori, E.; Sawa, H.; Okada, H.; Tobita, H.; Kasama, Y.; Kitaura, R.; Shinohara, H. *Angew. Chem., Int. Ed.* **2012**, *51*, 3377.

[3] (a) Matsuo, Y.; Okada, H.; Maruyama, M.; Sato, H.; Tobita, H.; Ono, Y.; Omote, K.; Kawachi, K.; Kasama, Y. *Org. Lett.* **2012**, *14*, 3784. (b) Kawakami, Y.; Okada, H.; Matsuo, Y. *Org. Lett*. **2013**, 15, 4466.

[4] (a) Ikuma, N.; Susami, Y.; Oshima, T. *Eur. J. Org. Chem.* **2011**, 6452. (b) Oshima, T.; Kitamura,

H.; Higashi, T.; Kokubo, K.; Seike, N. *J. Org. Chem.* **2006**, *71*, 299.

[5] (a) Kräutler, B.; Maynollo, J. *Tetrahedron* **1996**, *52*, 5033. (b) Kräutler, B.; Miiller, T.; Maynollo, J.; Gruber, K.; Kratky, C.; Ochsenbein, C.; Schwarzenbach, D.; Bürgi, H.-B. *Angew. Chem. Int. Ed. Engl.* **1996**, *35*, 1204.

[6] Aoyagi, S.; Nishibori, E.; Sawa, H.; Sugimoto, K.; Takata, M.; Miyata, Y.; Kitaura, R.; Shinohara, H.; Okada, H.; Sakai, T.; Ono, Y.; Kawachi, K.; Yokoo, K.; Ono, S.; Omote, K.; Kasama, Y.; Ishikawa, S.; Komuro, T.; Tobita, H. *Nat. Chem.* **2010**, *2*, 678.

[7] Okada, H.; Matsuo, Y. *Full. Nanotub. Carbon Nanostruct.* **2013,** In press.

[8] (a) Osuna, S.; Moreta, J.; Cases, M.; Morokuma, K.; Solà, M. *J. Phys. Chem. A* **2009**, *113*, 9721‑9726. (b) Fernàndez, I.; Solà, M.; Bickelhaupt, F. M. *Chem. Eur. J.* **2013**, *19*, 7416.

[9] (a) Klopman, G. *J. Am. Chem. Soc*. **1968**, *90*, 223. (b) Salem, L. *J. Am. Chem. Soc.* **1968**, *90*, 543.

[10] (a) Zhang, X.; Romero, A.; Foote, C. S. *J. Am. Chem. Soc*. **1993**, *115*, 11024. (b) Zhang, X.; Foote, C. S. *J. Am. Chem. Soc.* **1995**, *117*, 4271. (c) Vassilikogiannakis, G.; Orfanopoulos, M. *J. Am. Chem. Soc.* **1997**, *119*, 7394. (d) Vassilikogiannakis,G.; Orfanopoulos, M. *Tetrahedron Lett*. **1997**, *38*, 4323. (e) Vassilikogiannakis, G.; Chronakis, N.; Orfanopoulos, M. *J. Am. Chem. Soc*. **1998**, *120*, 9911. (f) Vassilikogiannakis, G.; Hatzimarinaki, M.; Orfanopoulos, M. *J. Org. Chem*. **2000**, *65*, 8180. (g) Vassilikogiannakis, G.; Orfanopoulos, M. *J. Org. Chem.* **1999**, *64*, 3392.

[11] Eyring, H. *J. Chem. Phys*. **1935**, *3*, 107.

[12] Yates, P.; Eaton, P. *J. Am. Chem. Soc*. **1960**, *82*, 4436.

Chapter 3:

Ionic conductivity of $[Li^+@C_{60}](X^-)$ in organic solvents and its electrochemical reduction to $Li^+@C_{60}^{\bullet-}$

As mentioned in general introduction, the most remarkable property of $[Li^+@C_{60}]$ salt is its high ionicity resulting from the encapsulated lithium cation. Although this ionic nature of $[Li^+@C_{60}](PF_6^-)$ is stated to be responsible for its rock-salt-type crystal structure, no other details on the effects of ionicity have been reported so far. In chapter 3, the ionic conductivity of $Li^+@C_{60}$ salts in organic solvents and the application of the ionic property for an electrochemical procedure to synthesize Li^+-encapsulated fullerene radical anion are described.

1. Introduction

One of the major ionic properties is "ionic conductivity" in solution phase.[1] An appropriate ion pair in solvents can electrically connect anode with cathode, and is called electrolyte. Electrochemical procedures for organic synthesis have attracted much attention due to its simple principle and environmental harmoniousness especially in fullerene chemistry but are not applicable without supporting electrolytes such as tetrabutylammonium salts.

On the other hand, the fullerene radical anion has been recognized as an intriguing material because of its unique electronic properties such as (super)conductivity and ferromagnetism.[2,3] In addition, the radical anion can serve as an important reaction intermediate for various unique chemical modifications of the fullerene cage.[4] Although many methods for the preparation of empty C_{60} radical anion salts have been reported, studies on endohedral fullerene radical anions are relatively stagnant.[5]

The author herein reports the high ionic conductivity of two types of Li^+-encapsulated fullerene in organic solvents, which has enabled a facile electrochemical synthesis of radical anion

($Li^+@C_{60}^{\bullet-}$) without any supporting electrolyte.

2. Results and Discussion

The measurement was carried out for two Li^+-encapsulated fullerenes, PF_6^- and NTf_2^- salt. The NTf_2^- salt was prepared by reported anion exchanging method for PF_6^- salt which was purchased form Idea International Corporation. Due to the solubility limitation and electrochemical stability, o-DCB was used as solvent for both salts, as well as CH_2Cl_2 only for NTf_2^- salt.

The molar conductivity Λ is defined as eqn (1),

$$\Lambda = \kappa / c \qquad (1)$$

where κ is the measured conductivity at each concentration (c). The Λ values for various concentrations of $Li^+@C_{60}$ salts are shown in Figure 1 and listed in Table 1, together with those of tetra-*n*-butylammonium hexafluorophosphate ($TBA^+PF_6^-$), which is commonly used as a supporting electrolyte in organic solvents. The exponential change in Λ with $c^{1/2}$ indicated that $[Li^+@C_{60}]$ salts

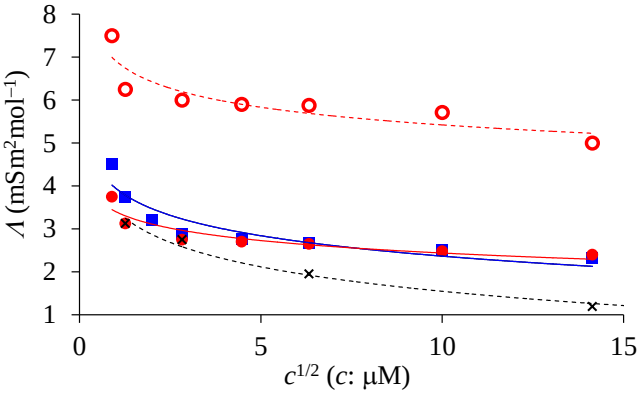

Figure 1. Molar conductivity of $[Li^+@C_{60}](PF_6^-)$ (square) and $[Li^+@C_{60}](NTf_2^-)$ (filled circle) measured in *o*-DCB at 298 K. The cross mark is the result of $TBA^+PF_6^-$ measured as a reference. The open circle is the result of $[Li^+@C_{60}](NTf_2^-)$ in CH_2Cl_2.

Table 1. Ionic conductivities of $[Li^+@C_{60}](PF_6^-)$, $[Li^+@C_{60}](NTf_2^-)$, and $TBA^+PF_6^-$ measured in *o*-DCB at 298 K.

c / μM	κ / mSm^{-1}	Λ / mSm^2mol^{-1}
$[Li^+@C_{60}](PF_6^-)$		
1.6	0.006	3.75
8	0.023	2.88
40	0.107	2.68
200	0.466	2.33
$[Li^+@C_{60}](NTf_2^-)$		
1.6	0.005 (0.010)[a]	3.13 (6.25)[a]
8	0.022 (0.048)[a]	2.75 (6.00)[a]
40	0.106 (0.235)[a]	2.65 (5.88)[a]
200	0.480 (0.480)[a]	2.40 (5.00)[a]
$TBA^+PF_6^-$		
1.6	0.005	3.13
8	0.22	2.75
40	0.078	1.95
200	0.238	1.19
empty C_{60}		
any	0	0

[a] Values in parentheses are measured in CH_2Cl_2 at 298 K.

themselves acted as weak electrolyte. As pristine C_{60} showed no ionic conductivity under the same conditions, the observed conductivity was regarded as a unique feature of the ion-encapsulated fullerene. The observed ionic conductivity of $Li^+@C_{60}$ salts in *o*-DCB were higher than that of $TBA^+PF_6^-$, indicating the weak interaction between the counter anion and encapsulated Li^+ even in such less polar solvent.

To discuss the ionizability of $[Li^+@C_{60}](PF_6^-)$, the electrostatic potential of the $Li^+@C_{60}$ cation and the distance between the cation and the PF_6^- anion at the most stable position were calculated by the density functional theory (DFT) at the B3LYP/6-31G* level (Figure 2). The result showed that the positive charge of $Li^+@C_{60}$ was not only located on the encapsulated Li^+ but also strongly delocalized on the carbon atoms of the C_{60} cage. Because of the thermal motion of the encapsulated Li^+ in the C_{60} cage, the charge delocalization might be more dynamically significant.[6] Furthermore, the Li–P distance of $[Li^+@C_{60}](PF_6^-)$ was calculated to be 5.65 Å, which was much longer than that in $LiPF_6$ (2.63 Å). This difference implied that the positional relationship observed between Li^+ and PF_6^- in $[Li^+@C_{60}](PF_6^-)$ is unusual in common ion pairs, indicating that the electrostatic attractive force between $Li^+@C_{60}$ and PF_6^- is weak due to the delocalized positive charge on the C_{60} cage and the distance limitation by this cage. This result is consistent with the previous report that the encapsulated Li^+ is in thermal motion at around room temperature even if $Li^+@C_{60}$ forms an ion pair with PF_6^-.[6]

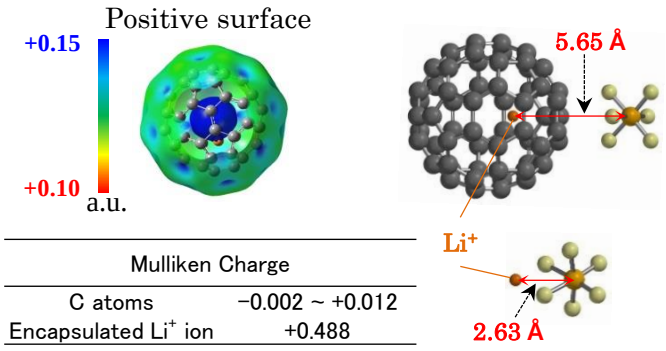

Figure 2. Electrostatic potential of the $[Li^+@C_{60}]$ cation (left) and the distance between encapsulated Li^+ and outer PF_6^- obtained by the theoretical calculation (B3LYP/6-31G*), the distances between Li^+ and P for $Li^+@C_{60}$ and $LiPF_6$, and Mulliken charges on C and Li^+ atoms of the $[Li^+@C_{60}]$ cation.

Moreover, the solvation effect is also important for the ion pair formation.[7] Because C_{60} is a

π-conjugated molecule, there must be strong π-π interaction between the cage and the aromatic solvent molecules, and the solvation can stabilize the ionized $Li^+@C_{60}$ cation.[8] Thus, $[Li^+@C_{60}](PF_6^-)$ shows high ionic conductivity, being used as a unique electrolyte which can be used in low-polarity aromatic solvents despite its high ionicity.

Based on the above results, we attempted to synthesize the Li^+-encapsulated fullerene radical anion electrochemically without using any supporting electrolyte. All synthetic process was carried out under N_2 atmosphere. The synthetic scheme is shown in Figure 3.

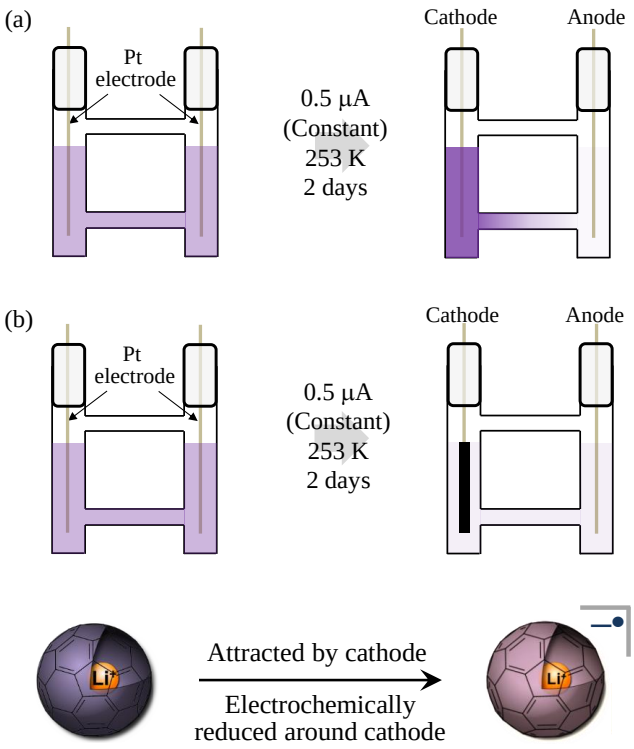

Figure 3. Pattern diagram of the electrochemical reduction of $[Li^+@C_{60}]$ cation in *o*-DCB (a) and CH_2Cl_2 (b).

An *o*-DCB solution of $[Li^+@C_{60}](PF_6^-)$ or a CH_2Cl_2 solution of $[Li^+@C_{60}](NTf_2^-)$ (ca. 0.29 mM) were used for the experiments. The solution was taken in an H-type cell, cooled to 253 K, and electrolyzed using a Pt electrode at a constant current (0.5 μA) for 2-3 days. In the case of *o*-DCB solution of $[Li^+@C_{60}](PF_6^-)$, homogeneous purple solution gradually became gradated because of ion conduction by $Li^+@C_{60}$ and PF_6^-. The cation was electrochemically reduced at the cathode, and a monovalent anion radical of Li^+-encapsulated fullerene $Li^+@C_{60}^{\bullet-}$ was selectively formed. However, because the product was also soluble in *o*-dichlorobenzene and any isolation procedures could not be applied for the purification, the generated product could not be separated from starting $[Li^+@C_{60}](PF_6^-)$. On the other hand, in the case of CH_2Cl_2 solution of $[Li^+@C_{60}](NTf_2^-)$, due to the lower solubility of the product for the solvent used, only the product was deposited on the surface of cathode.

The generated $Li^+@C_{60}^{\bullet-}$ was characterized by UV-vis-NIR, ESR, Raman, and NMR spectroscopy. The UV-vis-NIR spectrum of the o-DCB solution of deposit collected from the cathode is shown in Figure 4, along with the spectrum of the starting $[Li^+@C_{60}](PF_6^-)$ solution. The absorption maximum observed at 1035 nm was clearly assignable to the monovalent anion radical of the Li^+-encapsulated C_{60}.[9] In the case of *o*-DCB solution of $[Li^+@C_{60}](PF_6^-)$ used as starting solution, although the solution collected from cathode side showed the same absorption at 1035 nm, the estimated conversion to desirable radical species with reference to molar absorbance coefficient of empty C_{60} monovalent radical anion reported was ca. 30 %.[10] The generation of $Li^+@C_{60}^{\bullet-}$ was also confirmed by ESR measurement for

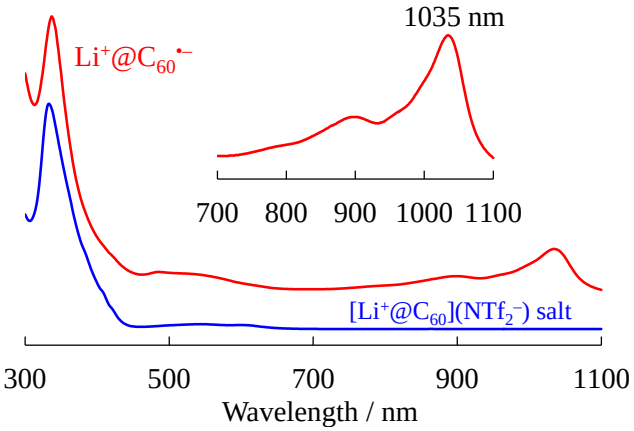

Figure 4. UV-vis-NIR absorption spectra of the product solution by electrochemical reduction of $[Li^+@C_{60}](NTf_2^-)$ and starting $[Li^+@C_{60}](NTf_2^-)$ solution in *o*-DCB. The inset is the expanded view of the NIR region of the spectrum of the product.

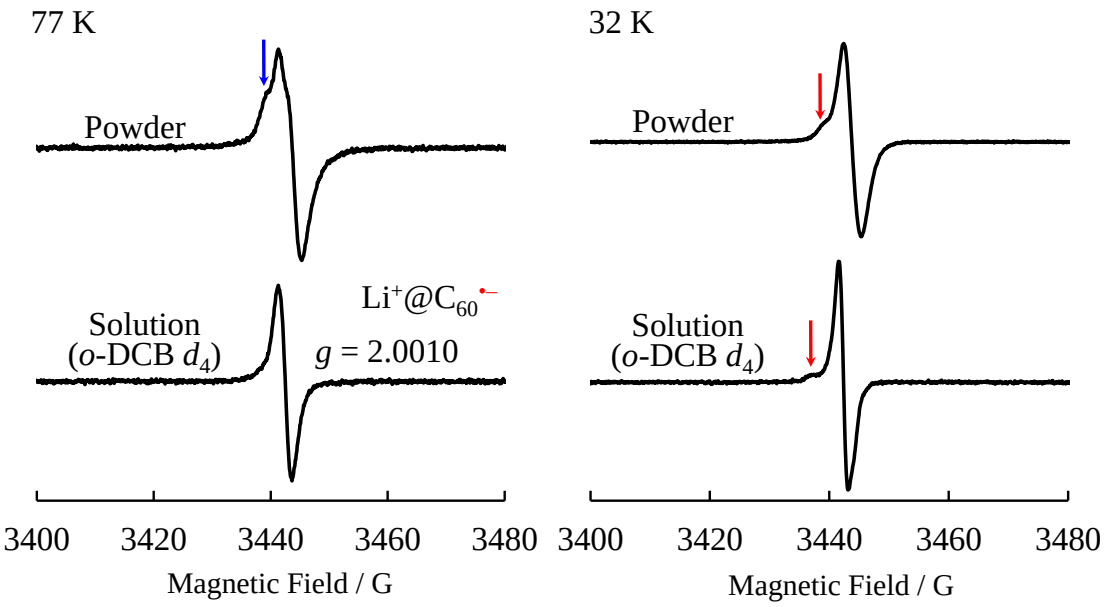

Figure 5. ESR spectra of the product measured for the collected solid and its *o*-DCB(d_4) solution at 77 K (left) and 32 K (right).

the *o*-DCB solution of the product at 77 K (Figure 5). The observed *g* value (2.0010) clearly indicated that the monovalent anion radical was exclusively produced through one-electron reduction.[9] On the other hand, in the spectra measured for the solid sample at 32 K, the line shapes were somewhat different from the result of o-DCB solution at 77 K (Figure 5). Considering the deferent density of the molecules in solid and solution, the observed splitting of the signal on the measurement for the solid at 77 K, dipole-dipole interaction between the radical molecules caused such signal changing. In the case of the measurement at lower temperature, the triplet dimer may be slightly formed and the species showed different ESR signals. The details of research on these results were now in progress. And at the low temperature below 77 K, the thermal motion of the encapsulated Li^+ may be stopped, and thus, the spectrum showed a sharp signal. The calculated spin density of $Li^+@C_{60}^{\bullet-}$ for the optimized structure indicated that the delocalized spin density is somewhat close to the encapsulated Li^+. However, because of the small hyperfine coupling constant of the ^7Li species, the interaction between the encapsulated Li^+ and the spin centre could not be evidenced from the spectrum. The electron nuclear double resonance (ENDOR) spectrum was attempted to measure such interaction, but showed no meaningful signals in our experiment. Raman spectrum of the product also indicated one electron reduction of fullerene cage as shown in Figure 6. The signals of Li^+-encapsulated fullerene salts observed at 1465 cm^{-1} were the "pentagonal pinch mode" known as an indicator of electron doping to [60]fullerene cage.[11] The observed red shift (ca. 9 nm) resulting from the decrease in average bond order suggested the generation of the monovalent radical anion cage. The $Li^+@C_{60}^{\bullet-}$ seems to be more stable as

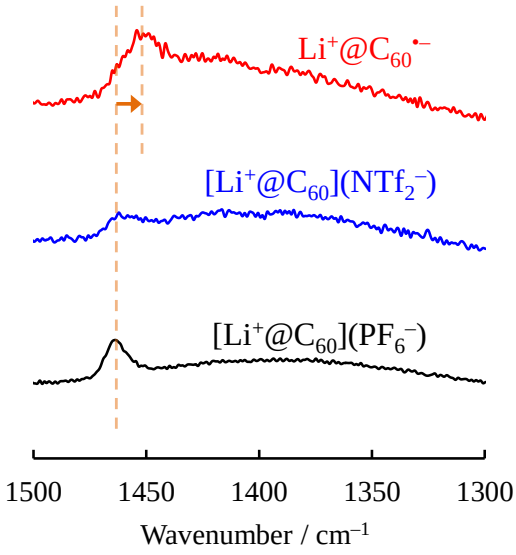

Figure 6. Raman spectra of the product, $[Li^+@C_{60}](NTf_2^-)$ and $[Li^+@C_{60}](PF_6^-)$ solids. Spectra were recorded using 532 nm excitation.

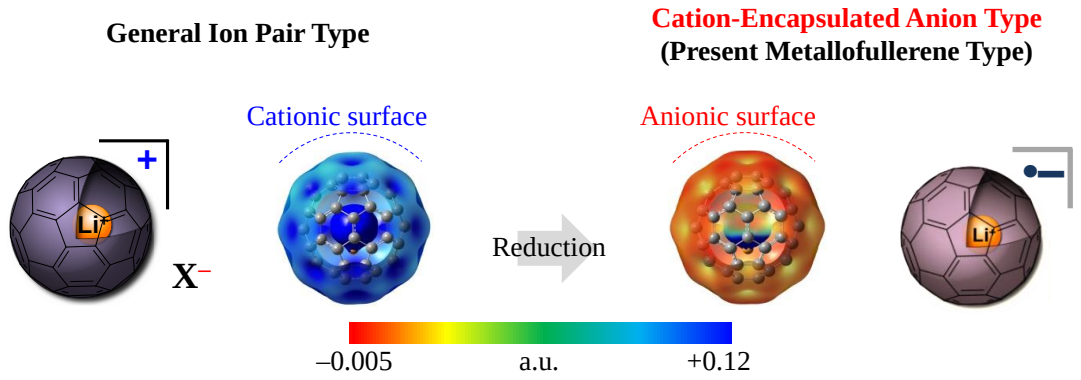

Mulliken Charge	
C atoms	-0.002 ~ +0.012
Encapsulated Li^+ ion	+0.488

Mulliken Charge	
C atoms	-0.022 ~ -0.002
Encapsulated Li^+ ion	+0.458

Figure 7. Calculated electrostatic potential (B3LYP/6-31G* method) of $Li^+@C_{60}$ (left) and $Li^+@C_{60}^{\bullet-}$ (right). $Li^+@C_{60}^{\bullet-}$ had a slightly negative potential on the C_{60} cage. In order to simplify the map, the range was set in –0.005 to +0.12.

compared with empty $C_{60}^{\bullet-}$. It is well known that empty C_{60} anions (C_{60}^{n-}, n = 1-6) are quite sensitive for air (O_2, H_2O) probably due to the electron transfer from the anions to O_2 or the nucleophilic addition of H_2O to fullerene cage, and thus the anions are immediately deactivated or degraded.[5] On the other hand, the $Li^+@C_{60}^{\bullet-}$ was detected by vis-NIR spectroscopy after 2 days from the exposure to the air. Because $Li^+@C_{60}$ has 0.7 eV lower LUMO level as compared with empty C_{60}, the electron transfer from reduced $Li^+@C_{60}^{\bullet-}$ to O_2 is less favorable than in the case of empty molecule. Of course the $Li^+@C_{60}^{\bullet-}$ is quite stable under inert atmosphere.

The two species could be clearly distinguished from each other on the basis of the calculated electrostatic potential (Figure 7). This result indicated that the chemical reactivity of the two types of Li^+-encapsulated fullerenes, such as the external-counter-anion-type (ion-pair-type) $[Li^+@C_{60}](PF_6^-)$ and the cation-encapsulated-anion-type (general endohedral fullerene-type) $Li^+@C_{60}^{\bullet-}$, are much different, and hence, $Li^+@C_{60}^{\bullet-}$ is a potential nucleophilic reactant for unique chemical transformations.

3. Conclusion

In conclusion, the ionic conductivity of Li^+-encapsulated [60]fullerene salts $[Li^+@C_{60}](PF_6^-)$ and $[Li^+@C_{60}](NTf_2^-)$ was measured in two organic solvents, *o*-DCB and CH_2Cl_2. $Li^+@C_{60}$ salts showed higher ionic conductivity than $TBA^+PF_6^-$ in *o*-DCB, indicating the possibility of electrochemical applications even in the absence of any supporting electrolyte. Furthermore, the Li^+-encapsulated [60]fullerene monovalent anion radical $Li^+@C_{60}^{\bullet-}$ was synthesized selectively by a very facile electrochemical method. Further studies on the use of anion-exchanged $Li^+@C_{60}$, application of $Li^+@C_{60}$ salts as a unique electrolyte, and derivatization via the anion species are now in progress, in addition to the synthesis and characterization of multivalent anions.

4. Experimental Section

General Procedure

$[Li^+@C_{60}](PF_6^-)$ was obtained from Idea International Corporation and used after purification by recrystallization from chlorobenzene/acetonitrile. $[Li^+@C_{60}](NTf_2^-)$ (anion-exchanged sample) was prepared by the reported procedure.[12] All other reagents were commercially available and used without further purification. Ionic conductivity measurement was performed by a HORIBA ES-51. UV-visible-NIR spectra were recorded on a Shimadzu UV-1800 spectrometer. ESR spectrum was measured on a JEOL JES-FA100. YAZAWA CS-12Z constant current regulator was used for electrochemical synthesis of $Li^+@C_{60}^{\bullet-}$. The ^7Li, ^1H, ^{13}C and ^{19}F nuclear magnetic resonance (NMR) spectra were recorded at 233.12 MHz, 599.85 MHz, 150.84 MHz and 564.23 MHz, respectively on a Varian Unity Inova 600.

Ionic conductivity measurement

$[Li^+@C_{60}](X^-)$ (X = PF_6 and NTf_2) (1.00 μmol) was dissolved in 5.00 mL of *o*-dichlorobenzene (*o*-DCB) or dichloromethane (CH_2Cl_2). These solutions (200 μM) were diluted to 100, 40, 20, 8, 4,

and 1.6 μM by each solvent under N_2 atmosphere, and then the ionic conductivity was measured 3 times. The measurement for the reference tetrabutylammonium hexafluorophosphate $TBAPF_6$ was carried out by the same procedure.

Electrochemical Synthesis of $Li^+@C_{60}^{\bullet-}$

An *o*-DCB or CH_2Cl_2 solution of $[Li^+@C_{60}](X^-)$ (ca. 0.29 mM) was taken in an H-type cell, cooled to 278 K, and electrolyzed using a Pt electrode at a constant current (0.5 μA) for 2–3 days under N_2 atmosphere. The $Li^+@C_{60}^{\bullet-}$ was produced around cathode as redish purple solution or on cathode as black precipitate.

References for Chapter 3

[1] Marcus, Y.; Hefter, G. *Chem. Rev*. **2006**, *106*, 4585.

[2] (a) Tanigaki, K.; Hirosawa, I.; Ebbesen, T. W.; Mizuki, J.; Shimakawa, Y.; Kubo, Y.; Tsai, J. S.; Kuroshima, S. *Nature* **1992**, *356*, 419. (b) Ganin, A. Y.; Takabayashi, Y.; Jeglič, P.; Arčon, D.; Potočnik, A.; Baker, P. J.; Ohishi, Y.; McDonald, M. T.; Tzirakis, M. D.; Mclennan, A.; Darling, G. R.; Takata, M.; Rosseinskym M. J.; Prassides, K. *Nature* **2010**, *466*, 221. (c) Moriyama, H.; Kobayashi, H.; Kobayashi A.; Watanabe, T. *J. Am. Chem. Soc*. **1993**, *115*, 1185.

[3] Stephens, P. W.; Cox, D.; Lauher, J. W.; Mihaly, L.; Wiley, J. B.; Allemand, P.-M.; Hirsch, A.; Holczer, K.; Li, Q.; Thompson, J. D.; Wudl, F. *Nature*, **1992**, *355*, 331.

[4] Kokubo, K.; Arastoo, R. S.; Oshima, T.; Wang, C. C.; Gao, Y.; Wang, H. L.; Geng, H.; Chiang, L. Y. *J. Org. Chem*. **2010**, *75*, 4574.

[5] Reed, C. A.; Bolskar, R. D. *Chem. Rev*. **2000**, *100*, 1075.

[6] Aoyagi, S.; Sado, Y.; Nishibori, E.; Sawa, H.; Okada, H.; Tobita, H.; Kasama, Y.; Kitaura, R.; Shinohara, H. *Angew. Chem. Int. Ed.* **2012**, *51*, 3377.

[7] Marcus, Y.; Hefter, G. *Chem. Rev*. **2006**, *106*, 4585.

[8] Oshima, T.; Mikie, T.; Ikuma, N.; Yakuma, H. *Org. Biomol. Chem*. **2010**, *10*, 1730.

[9] (a) Fukuzumi, S.; Ohkubo, K.; Kawashima, Y.; Kim, D. S.; Park, J. S.; Jana, A.; Lynch, V. M.; Kim, D.; Sessler, J. L. *J. Am. Chem. Soc.* **2011**, *133*, 15938. (b) Ohkubo, K.; Kawashima, Y.; Fukuzumi, S. *Chem. Commun.* **2012**, *48*, 4314.

[10] Heath, G. A.; McGrady, J. E.; Martin, R. L. *J. Chem. Soc., Chem. Commun*. **1992**, 1272.

[11] (a) McGlashen, M. L.; Blackwood, M. E. 'Jr.; Spiro, T. G. *J. Am. Chem. Soc.* **1993**, *115*, 2074. (b) Sanguinetti, S.; Benedek, G. *Phys. Rev. B* **1994**, *50*, 15439.

[12] Okada, H.; Matsuo, Y. *Full. Nanotub. Carbon Nanostruct.* **2013,** In press.

Conclusions

The present thesis deals with the development of fundamental chemistry of lithium cation-encapsulated fullerene $Li^+@C_{60}$ focused on the derivatizations, kinetic study, and ionic property. The results obtained through the studies and described in this thesis are summarized as below:

Chapter 1 described the synthesis of novel Li^+-encapsulated fullerene derivative, Li^+-encapsulated multihydroxylated fullerene, and its characterization. In the case of $Li@C_{60}$ cluster used as a starting material, the solubility was drastically enhanced by the hydroxylation. And when the purified $[Li^+@C_{60}](PF_6^-)$ was used, the hydroxylation was site-selective to give a single major isomer (ca. 70%) with two minor isomers in marked contrast to the case of $Li@C_{60}$ cluster. From the analysis of radical species produced as a reaction intermediate on the stage of electron oxidation by fuming sulfuric acid, this unusual site-selective hydroxylation was caused by the lower HOMO level of lithium encapsulated fullerene than that of empty C_{60}. This result suggests that the metal encapsulated fullerenes are capable to become a new-type of fullerene multi-adducts with appreciable site-selectivity.

In chapter 2, Diels-Alder product $[Li^+@C_{60}(C_6H_8)](PF_6^-)$ was synthesized by the facile reaction of Li^+-encapsulated fullerene with 1,3-cyclohexadiene. The kinetic study revealed that the Diels-Alder reaction was ca. 2400 times faster than that of empty C_{60} because of the increased interaction by the lower-lying LUMO of $Li^+@C_{60}$ with the HOMO level of C_6H_8. The remarkable rate enhancement was rationalized by 24 kJ/mol smaller activation energy which was estimated by Arrhenius and Eyring plots as well as other kinetic parameters such as $\Delta H^{\ddagger}$, $\Delta S^{\ddagger}$, and $\Delta G^{\ddagger}$. In addition, the results were confirmed by theoretical calculations and the reaction was considered as "encapsulated Li^+-mediated" DA reaction.

Chapter 3 described the results of the ionic conductivity measurements for the two kinds of $Li^+@C_{60}$ salts, $[Li^+@C_{60}](PF_6^-)$ and $[Li^+@C_{60}](NTf_2^-)$. The observed ionic conductivity in o-dichlorobenzene was higher than that of tetrabutylammonium hexafluorophosphate $TBA^+PF_6^-$ which is a common supporting electrolyte for any organic solvents. The results indicated that $Li^+@C_{60}$ salts can be applied to electrochemical procedures as a supporting electrolyte. Based on the observed conductivity, $Li^+@C_{60}$ monovalent radical anion $Li^+@C_{60}^{\bullet-}$ was synthesized by facile electrochemical synthesis and characterized mainly by ESR and Raman Spectroscopy. The obtained $Li^+@C_{60}^{\bullet-}$, the second type of Li^+-encapsulated fullerenes described as the cation-encapsulated-anion-type (general endohedral fullerene-type), may have unique electron conducting properties that are different from the present external-counter-anion-type (ion-pair-type) of Li^+-encapsulated fullerene.

List of Publications

1) Synthesis of a Lithium-Encapsulated Fullerenol and the Effect of the Internal Lithium Cation on Its Aggregation Behavior

Hiroshi Ueno, Yuji Nakamura, Naohiko Ikuma, Ken Kokubo, Takumi Oshima

Nano Res. **2012**, *5*, 558-564.

2) Synthesis of a New Class of Fullerene Derivative $Li^+@C_{60}O^-(OH)_7$ as a "Cation–Encapsulated Anion Nanoparticle"

Hiroshi Ueno, Ken Kokubo, Eunsang Kwon, Yuji Nakamura, Naohiko Ikuma, Takumi Oshima

Nanoscale **2013**, *5*, 2317-2321.

3) Ionic Conductivity of $[Li^+@C_{60}](PF_6^-)$ in Organic Solvents and its Electrochemical Reduction to $Li^+@C_{60}^{\bullet-}$

Hiroshi Ueno, Ken Kokubo, Yuji Nakamura, Kei Ohkubo, Naohiko Ikuma, Hiroshi Moriyama, Shunichi Fukuzumi, Takumi Oshima

Chem. Commun. **2013**, *49*, 7376-7378.

4) Kinetic Study in Diels–Alder Reaction of $Li^+@C_{60}$ with Cyclohexadiene: Enhanced Reactivity Promoted by Encapsulated Li^+

Hiroshi Ueno, Hiroki Kawakami, Koji Nakagawa, Hiroshi Okada, Naohiko Ikuma, Shinobu Aoyagi, Ken Kokubo, Yutaka Matsuo, Takumi Oshima

J. Am. Chem. Soc. In preparation

List of Supplementary Publications

1) Magic Number Effect on Cluster Formation of Polyhydroxylated Fullerenes in Water–Alcohol Binary Solution

Yuji Nakamura, Hiroshi Ueno, Ken Kokubo, Naohiko Ikuma, Takumi Oshima

J. Nanopart. Res. **2013**, *15*, 1755-1761.

2) Radical-Scavenging Ability of Hydrophilic Carbon Nanoparticles: From Fullerene to its Soot

Ken Kokubo, Shizuka Yamakura, Yuji Nakamura, Hiroshi Ueno, Takumi Oshima

Full. Nanotub. Carbon Nanostruct. **2013**, *in press.*

3) Effect of Functional Group Polarity on the Encapsulation of C_{60} Derivatives in the Inner Space of Carbon Nanohorns

Keita Kobayashi, Hiroshi Ueno, Ken Kokubo, Masako Yudasaka, Hidehiro Yasuda

Carbon **2013**, *68*, 345-361.

Acknowledgements

The author would like to express his heartfelt gratitude to Professor Dr. Takumi Oshima, Division of Applied Chemistry, Graduate School of Engineering, Osaka University, for his continuous guidance, invaluable suggestions, and science encouragement throughout the work.

The author is indebted to Associate Professor Dr. Ken Kokubo, Division of Applied Chemistry, Graduate School of Engineering, Osaka University, for his continuous guidance and stimulating discussions for carrying out this work.

The author also wishes to make a grateful acknowledgement to Assistant Professor Dr. Naohiko Ikuma, Division of Applied Chemistry, Graduate School of Engineering, Osaka University, for his helpful suggestions and heartfelt advice.

The author wishes to express his deeply thanks Professor Dr. Hiroshi Uyama, Professor Dr. Toshikazu Hirao, and Professor Dr. Satoshi Minakata for their reviewing this dissertation with helpful comments and suggestions.

The author would like to thank Professor Dr. Shunichi Fukuzumi for his valuable suggestions and comments.

The author is grateful to Designated Associate Professor Dr. Kei Ohkubo for his helpful comments and stimulating discussions.

The author would like to thank Professor Dr. Hiroshi Moriyama, Department of Chemistry, School of Science, Toho University, for his ungrudging supports and helpful comments.

The author deeply thanks Assistant Professor Keita Kobayashi and Hidehiro Yasuda for helpful guidance on TEM observation.

The author is deeply grateful to Dr. Hiroshi Okada and Professor Dr. Yutaka Matsuo for their helpful suggestions and heartfelt advices.

The author wishes to thank Associate Professor Dr. Shinobu Aoyagi for the X-ray diffraction measurement.

The author is indebted to Assistant Professor Eunsang Kwon for his invaluable suggestions and stimulating discussion.

The author deeply thanks Professor Dr. Tatsuhisa Kato for ESR/ENDOR measurements and helpful guidance.

The author wishes to thank Mr. Yasuhiko Kasama and Mr. Kazuhiko Kawachi for their ungrudging supports and stimulating discussions.

The author is indebted to Emeritus Professor Dr. Rikizo Hatakeyama for his helpful suggestion.

The author is grateful to Dr. Takami Akagi and Professor Dr. Mitsuru Akashi for DLS and zeta potential measurements, and to Assistant Professor Dr. Akinori Saeki and Professor Dr. Shu Seki for measurement of ESR spectra. The author is indebted to Assistant Professor Dr. Taro Uematsu and Professor Dr. Susumu Kuwabata for ICP-AES analysis. The author thanks Shimadzu Corp. and Nacalai Tesque Inc. for SPM analysis and the helpful guidance of HPLC, respectively. The author also thanks SPring-8 with the approval of the Japan Synchrotron Radiation Research Institute (JASRI) for the X-ray diffraction measurement.

The author is deeply indebted to all members of Oshima Laboratory (Area of Physical Organic Chemistry) for their hearty encouragement, constant support and assistance. Thanks are also due to the Instrumental Analysis Center, Graduate School of Engineering, Osaka University, for the measurement of NMR spectra, MALDI/FAB mass spectra, and elemental analysis.

Finally, the author is deeply grateful to his family, Nobuo Ueno, Setsuko Ueno and Takeshi Ueno for their full understanding and perpetual support.